physician told Prof. Okinaka that the patient was suffering from muscular dystrophy, based on the serum aldolase activities that Sugita measured. Prof. Okinaka became furious and told Sugita that it was not acceptable to make a diagnosis simply on the determination of something in the blood. In retrospect, Prof. Okinaka was correct; the patient was probably suffering from polymyositis rather than muscular dystrophy.

However, the incident led to one of the monumental achievements in the history of muscular dystrophy research due to the outstanding professional intuition of Dr. Setsuro Ebashi. When Dr. Momoi, a close friend of Dr. Ebashi since middle school, told him about the serum aldolase activity in muscular dystrophy, he pointedly asked Dr. Momoi, "Why do you determine a nonspecific enzyme such as aldolase in muscular diseases? You should look at the level creatine phosphokinase, which is more specific to skeletal muscle than aldolase." It was a stroke of genius! At his suggestion, we set up a team, headed by Dr. Ebashi and including Drs. Momoi, Toyokura, and Sugita, to study creatine phosphokinase (CPK; it was also known as creatine kinase or CK). Thus, first paper on serum CK activity in progressive muscular dystrophy was published by Ebashi and coworkers in 1959.[8] Among various neuromuscular disorders, they found increased serum CK levels in patients with muscular dystrophy, and it is now regarded as the most reliable laboratory test for muscular dystrophy. The discovery of the importance of serum CK opened the door for the recent myology research, in particular pathological studies including genetics and the exploration of treatments such as gene therapy.

Discovery of dystrophin and its localization at the muscle surface membrane

A pioneer application of positional cloning to human diseases appeared in 1986, when the gene responsible for DMD/Becker muscular dystrophy (BMD) was isolated by Dr. A.P. Monaco *et al.* of Dr. L. Kunkel's group.[3] The *DMD* gene is 2,500 kb long and consists of 79 exons covering 1% of the x-chromosome. It is transcribed to yield a 14 kb cDNA. In 1987, Dr. E.P. Hoffman *et al.* identified a 427 kD protein encoded by the *DMD* gene, and this protein was named "dystrophin",[4] which is absent from the skeletal muscle of most patients with DMD. Almost all cases of DMD showed an out-of-frame mutation. In contrast, most patients with BMD had an in-frame mutation. Using polyclonal antibodies against the near N-terminal portion derived from the dystrophin cDNA, Dr. Kiichi Arahata *et al.* of the muscular dystrophy research group at National Institute of Neuroscience, National Center of Neurology and Psychiatry, Japan, identified a specific immunohistochemical reaction with peptides on the surface membrane of skeletal and cardiac muscle fibers that was absent in the muscles of DMD patients.[9] These results have been confirmed by other research groups. In symptomatic carriers of DMD, a distinct mosaic pattern of immunohistochemical staining of the surface membrane of the muscle fibers can be observed. BMD exhibits a positive but faint and patchy expression pattern of dystrophin with altered protein contents and molecular weights. Thus, it became clear that DMD and BMD are caused by fragility of the muscle surface membrane due to the lack of dystrophin.

Development of therapy for DMD

Drug treatment for DMD patients is currently restricted almost completely to corticosteroids (oxandrolone and prednisone), but a variety of therapeutic approaches to muscular dystrophies have been tested over the past few decades, and some of them show great promise (recently reviewed in Ref. 10, and current situation was summarized in Table 1). For successful application of viral vector-mediated gene therapy, there are still several hurdles to be overcome.[11] Pluri- or multipotent stem cell-based therapies are still in their immature stages, but currently some alternatives are progressing to clinical trials. Among several therapeutic approaches in preclinical or clinical stage, authors here focus on one of the most promising therapeutic approaches: exon skipping with antisense oligonucleotides (AOs).

Exon-skipping therapy using AOs

DMD is caused by the lack of dystrophin, most commonly as a result of frame-shift mutations. Deletions and duplications in the *DMD* gene result in out-of-frame mRNA, such as nonsense mutations in which a single base change alters a codon into a premature stop codon. Theoretically, in these cases, selective removal of the flanking exons can result in an in-frame mRNA transcript. Such an in-frame mRNA transcript can be translated into a quasi-dystrophin protein (reviewed in Ref. 12). AOs, which hybridize the sequences near the splice acceptor or donor sites as well as within exons, can alter gene expression *via* steric block interference with the splicing machinery, and thereby direct the exclusion

Table 1. Clinical trials for DMD/BMD

Category	Interventions	Phase (ClinicalTrials.gov)
Drug	**Myostatin blocking**	
	MYO-029	Completed; not effective
	Read-through	
	PTC124	Completed; not effective
	Gentamicin	Completed; not effective
	Others	
	Pentoxifylline	Completed; not effective
	Idebenone	Phase III
	Ramipril vs. Carvedilol	Phase IV
	Coenzyme Q10 and prednisone	Phase III
	Coenzyme Q10 and lisinopril	Phase II/III
	Debio-025 (cyclosporine analogue)	Phase IIb
Gene therapy	**Exon skipping** (systemic delivery)	
	PRO051 (2′-*O*-MePS AO)(exon 51 skipping)	Phase III
	PRO044 (2′-*O*-MePS AO)(exon 44 skipping)	Phase I/II
	AVI-4658 (PMO)(exon 51 skipping)	Phase IIb
	AAV vector	
	rAAV2.5-CMV-Mini-Dystrophin	Phase I*
Cell therapy	**Satellite cells (myoblasts)**	Pending
	Mesoangioblasts	In preparation
	Induced pluripotent stem (iPS) cells	Experimental

Shown are representative ongoing or just finished clinical trials for DMD. Some have finished with disappointing results. For more information, please refer to the homepage presented by the U.S. National Institute of Health, 'ClinicalTrials.gov'.
*Unwanted immune responses to dystrophin have been reported at the 2010 meeting of the American Academy of Neurology (http://quest.mda.org/news/caution-immune-response-seen-dmd-gene-therapy).

of one or more exons in the final transcript, resulting in restoration of the reading frame of dystrophin mRNA and the expression of a shorter, truncated but functional dystrophin.

One of the pioneering researchers who tried to restore the reading frame of the mutated DMD transcripts was Dr. Masafumi Matsuo at Kobe University.[13] His group tried to skip exon 19 of the *DMD* gene in exon 20-deleted DMD patients, based on the idea of DMD Kobe, where exon 19 has been skipped due to a 52-bp deletion within the exon. Later, proof-of-concept studies by many groups followed *in vitro* and *in vivo* (reviewed in Ref. 14).

Chemistries of AOs

For maximal effects in exon-skipping therapy, the chemistry of AOs seems to be one of most critical factors. AOs used for exon skipping are usually 20–25 bases long and chemically synthesized. Various chemistries for AOs have been proposed to overcome the unstable nature of single-strand DNA or RNA molecules. Several modifications of AOs include bicyclic locked nucleic acid (LNA), peptide nucleic acid (PNA), ethylene-bridged nucleic acid (ENA), 2′-*O*-methyl phosphorothioate AO (2′-*O*-MePS AO), and phosphorodiamidate morpholino oligomer (PMO). Among them, 2′-*O*-MePS AO and PMO are the most frequently utilized because of their suitable properties (Fig. 1).

2′-*O*-MePS AO. The structure of 2′-*O*-MePS AO is similar to that of RNA, but it is methylated at the 2′-OH position of the ribose ring. 2′-*O*-MePS AO is widely used because it is relatively easy to synthesize and cheap to produce. 2′-*O*-MePS AO is stable, has a high affinity to mRNA, and is also resistant to nucleases, however the low solubility of 2′-*O*-MePS AO in water prevents its use at higher dosages.

PMO. PMO has a morpholine ring instead of a deoxyribose ring in DNA, and these artificial rings

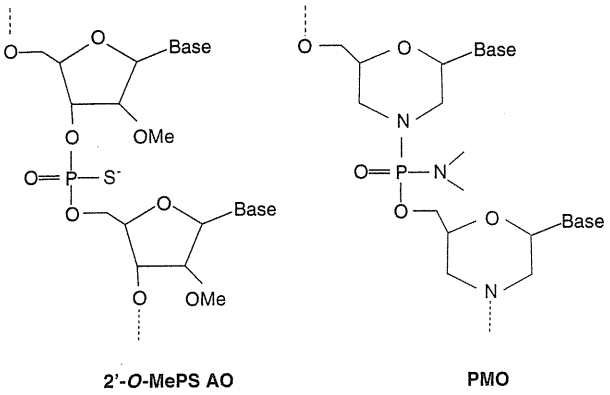

Fig. 1. Comparison of chemistry used in clinical trials. 2′-*O*-MePS AO: 2′-*O*-methyl phosphorothioate antisense oligonucleotides. PMO: phosphorodiamidate morpholino oligomers. PMO (AVI BioPharma, http://www.avibio.com/) has a different backbone (morpholino backbone) from RNA or DNA, enabling highly sequence-specific, stronger base pairing to the target RNA than RNA or DNA. Red highlights the differences in the chemistry from RNA or DNA.

are linked to each other through phosphorodiamidate, enabling highly sequence-specific, stronger base pairing to the target RNA than RNA or DNA. Importantly, PMO does not stimulate or activate Toll-like receptors and therefore does not activate innate immune responses. In addition, PMO is believed to be not recognized by cellular proteins and to be resistant to nuclease-mediated degradation. PMO has high solubility in water.

Other chemicals to improve efficiencies of delivery to whole-body musculature. Delivery of AOs to normal tissues *in vivo* is generally difficult because healthy tissues do not take up PMO or 2′-*O*-MePS AO. Although the mechanisms are not fully understood, PMO can easily enter the nuclei of skeletal muscle of DMD patients. This might be because the dystrophin-deficient muscle membrane is inherently leaky due to absence of the dystrophin-glycoprotein complex.

However, systemic administration of 2′-*O*-MePS AO or PMO failed to restore dystrophin expression in the heart, although it is again unclear why cardiac cells do not take up 2′-*O*-MePS AO or PMO. To improve the efficacy of its introduction into cardiomyocytes, a PMO covalently conjugated with a designed cell-penetrating peptide (PPMO) was injected into dystrophin-deficient *mdx* mice. Systemic delivery of the novel PPMO restored dystrophin to almost normal levels in both cardiac and skeletal muscles in *mdx* mice.[15] Later, the same group reported that a PMO modified with an octaguanidinium dendrimer, Vivo-Morpholino, also restored dystrophin expression in cardiac and skeletal muscles.[16] So far, no study has clearly demonstrated toxicity after systemic delivery or immune response to PPMO or Vivo-Morpholino.

AOs designs

To obtain efficient exon skipping while lowering the dose of AOs for clinical trials, the design of the AOs (base sequence) is important. In eukaryotic organisms, the gene is transcribed in the nucleus and introns are spliced out into mRNA, and then the mRNA is exported from the nucleus to the cytoplasm. Therefore, AOs must either enter the nucleus, where they bind to their target pre-mRNA sequences and get in the way of molecules that are otherwise involved in the splicing process, or they must alter the secondary structure folding of the pre-mRNA. AOs targeting exon-intron boundary sequences can often effectively induce exon skipping. On the other hand, when web-based software, such as ESEfinder (http://rulai.cshl.edu/tools/ESE), is used to design AO sequences to target an ESE, exon skipping is not always induced. Recently, Wee *et al.* have developed bioinformatic tools to optimize AOs sequences based on the pre-mRNA secondary structure.[17] Nevertheless, no single design tool is sufficient for designing the AOs, and often empirical analysis is required.

Proof of principle of exon skipping therapy in animal models

Cultured skeletal muscle cells from DMD patients are often used to evaluate the exon-skipping efficiency of newly-designed AOs.[18] However, to assess the therapeutic benefits, preclinical studies must be performed using animal models. In this section, studies using *mdx* mice and dystrophic dogs are described and discussed.

Exon skipping in *mdx* mice. The *mdx* mouse is a naturally occurring animal model that has a nonsense mutation in exon 23 of the *DMD* gene, resulting in a premature stop codon and complete absence of dystrophin.[19] *Mdx* mice show high levels of serum CK, active muscle degeneration/regeneration cycles, and loss of myofibers and fibrosis in the diaphragm, but still show mild, non-progressive muscle weakness of the limbs and only 20% reduction in life span. In this point, *mdx* might not be an ideal animal model for DMD, but due to the low cost of maintenance and short gestation times, many preclinical studies have been carried out using *mdx* mice.

Lu *et al.* reported the local administration of the AOs with the non-ionic polymer F127, which promotes intracellular uptake of 2′-*O*-MePS AO, to the skeletal muscles of 2-week-old *mdx* mice. The result showed that dystrophin together with β-dystroglycan, sarcoglycans, and nNOS was restored in 20% of the muscle fibers.[20] Furthermore, systemic administration of anti-sequences of the same 2′-*O*-MePS AO with F127 revealed that dystrophin was expressed in the skeletal muscle of the whole body. 2′-*O*-MePS AO produced no toxicity, but its expression did not reach a therapeutic level.[21] Likewise, Wells *et al.* reported that local administration of 2′-*O*-MeAO using electroporation restored dystrophin expression to up to 20% of the normal level.[22] Systemic induction of dystrophin expression by PMO administration reached up to 20% in whole body skeletal muscle.[23]

Dystrophic dogs as models for DMD. Muscular dystrophy in dogs was originally identified in golden retrievers and designated "golden retriever muscular dystrophy" (GRMD). GRMD shows progressive skeletal muscle weakness and atrophy as well as abnormal electrocardiographic findings and myocardial fibrosis like those seen in DMD. Because the phenotype and genetic background are closer to human DMD than those of the mouse model, the dystrophic dog is a useful model to examine pathogenesis and therapeutic strategies. However, the dogs are too large to be maintained conveniently; thus, we have established a colony of medium-sized beagle-based dystrophic dogs (canine X-linked muscular dystrophy in Japan: $CXMD_J$) at the National Center of Neurology and Psychiatry, Tokyo, by using artificial insemination of frozen GRMD semen.[24] Still, we have found that $CXMD_J$ requires extra daily care, and therefore, is expensive.

Clinical features of $CXMD_J$. The level of serum CK in neonatal $CXMD_J$ is very high, and 25–33% of the pups die of respiratory failure during the neonatal period, mainly due to severe degeneration and thus dysfunction of the diaphragm. Around the age of 2–3 months, atrophy and weakness of limb muscles appear; then, gait disturbance, joint contracture, macroglossia, and dysphasia appear in rapid progression until the dogs are 10 months of age; subsequently, the progression is retarded.[24]

Cardiac involvement of dystrophic dogs. Dystrophic dogs and DMD have similar cardiac involvement, including distinct deep Q-waves on the electrocardiogram and fibrosis of the left ventricular wall. The distinct deep Q-waves are generally ascribed to fibrosis in the posterobasal region of the left ventricular wall in DMD, but one report suggests that the deep Q-waves precede the development of fibrosis in $CXMD_J$.[25] Importantly, Purkinje fibers in dystrophic dogs showed remarkable vacuolar degeneration despite the absence of detectable fibrotic lesions in the ventricular myocardium. In the degenerated Purkinje fibers, Dp71, a C-terminal truncated isoform of dystrophin, was up-regulated at the sarcolemma. In addition, the calcium-dependent protease μ-calpain was found at the cell periphery near the sarcolemma or in the vacuoles. Utrophin, a homologue of dystrophin, was also highly up-regulated in the Purkinje fibers in the early stage. Together, the selective degeneration of Purkinje fibers may be associated with distinct deep Q-waves on electrocardiograms and the fatal arrhythmia seen in dystrophinopathy.[25]

Multi-exon skipping in dystrophic dogs. The dystrophic dogs have a point mutation at the intron 6 splice acceptor site in the canine *DMD* gene, resulting in skipping of exon 7 and a premature stop codon in exon 8. Thus, dystrophin is not produced in the affected dog. Recently, Yokota *et al.* reported systemic administration of three PMOs targeting exons 6 and 8 to convert an out-of-frame mutation to an in-frame mutation in $CXMD_J$.[26] The result showed that dystrophin was restored in the entire body skeletal muscle. The authors reported that the motor ability of treated dystrophic dogs was improved and that they showed no side effects. To the best of our knowledge, this is the first report that multi exon-skipping is feasible and effective in improving performance of dystrophic animals *in vivo*.

As reported in *mdx* mice, a combination of PMOs failed to restore the expression of dystrophin in cardiac muscle, even at a high dose in $CXMD_J$. To resolve this problem, modified PMOs (PPMO or Vivo-Morpholino) were tested (Yokota *et al.*, unpublished observation).

Viral vector-mediated exon skipping

The duration of the effects of AOs *in vivo* is limited; therefore, patients have to be injected with AOs weekly or monthly to maintain the therapeutic levels of dystrophin. An alternative strategy is to deliver AOs *via* adeno-associated virus (AAV) vector-mediated gene transfer. Based on an AAV vector-mediated approach, Goyenvalle *et al.* linked U7 small nuclear RNA to antisense sequences to achieve sustained dystrophin expression derived from skipped mRNA for more than 13 weeks in the limbs

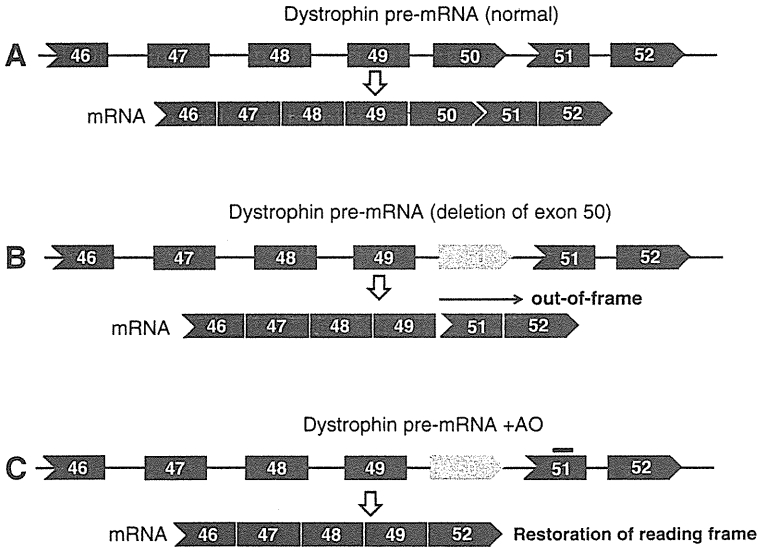

Fig. 2. Example of exon skipping therapy for DMD patients with deletion of exon 50. A. Normal dystrophin transcript and mRNA. B. Deletion of exon 50 disrupts the open reading frame, leading to a premature stop codon, unstable mRNA, and a truncated unstable protein. C. Targeted skipping of exon 51 using antisense oligonucleotides, such as AVI-4658 or PRO051 (blue line), restores the reading frame and produces a truncated but functional dystrophin that lacks exons 50 and 51.

of the *mdx* mouse.[27] Lentiviral vectors were also used to modify muscle stem cells expressing modified small nuclear RNAs that change splicing patterns of pre-mRNAs and correct the reading frame.[28),29]

Test of AOs efficacy using patient cells

To apply exon skipping therapy to individuals, not only the deletion pattern in the genome but also the mRNA/cDNA level must be analyzed to determine the precise splicing pattern and to design therapeutic AOs. Subsequently, designed AOs must be tested *in vitro* on cells derived from the patient before clinical trials. Skin fibroblasts are easy to obtain, but the levels of DMD transcripts are low, and therefore the results tend to be variable. On the other hand, preparation of myoblasts through biopsy from dystrophic patients is invasive. Therefore, transformation of fibroblasts to myoblasts *in vitro* by forced MyoD expression is often used to test the efficacy of AOs.[30),31]

Multiple exon skipping: theory and reality

We and other research groups tried to find the most effective target of exon skipping strategy among DMD patients. Theoretically, exon 51-skipping therapy is effective for up to 15% of DMD patients having a deletion, but large numbers of DMD patients will not benefit from it. We recently reported that three unrelated patients with a deletion of exons 45–55 showed very mild skeletal muscle involvement and were ambulant until his seventies in a patient.[32] Béroud *et al.* also described 15 asymptomatic or very mild patients with an exon 45–55 deletion.[33] In fact, the Leiden Muscular Dystrophy database indicates that the exon 45–55 deletion produced a BMD phenotype in more than 95% of the cases. Collectively, these observations indicate that approximately 60% of DMD patients having a deletion within the hot spot may be treatable with multi-exon skipping of exons 45–55. We recently tried exon 45–55 skipping by injection of a mixture of 10 PMOs in the anterior tibial muscle of *mdx*52 mice[34] and confirmed that multi-exon skipping is feasible, at least in mice (Aoki *et al.*, unpublished observation). However, the efficacy of multi-exon skipping was lower than that of single-exon skipping, possibly because many partially spliced products, many of which are again out-of-frame, are produced.

Phase I/II clinical trials of exon skipping for DMD

Based on the success of AOs-mediated exon skipping in animal models, clinical trials have been performed or are in progress for the skipping of exon 51 of the *DMD* gene (Fig. 2 and Table 1).

2′-*O*-MePS AO. Skipping of the exon 51 of the *DMD* gene with 2′-*O*-MePS AO, PRO051, has been already tested on DMD patients by a Dutch group.[35]

Four DMD patients received a dose of 0.8 mg of PRO051 injected into the tibialis anterior muscle. A biopsy performed 28 days later revealed restoration of sarcolemmal dystrophin in 64% to 97% of myofibers of each patient. Further, PRO051 did not evoke any clinically apparent adverse events.

PMO. Recently, a UK group reported that local injection of morpholino oligomer AVI-4658 successfully restored the expression of dystrophin in treated muscles of all seven DMD patients.[36] No adverse events related to AVI-4658 were observed. Based on these observations, systemic injection of AVI-4658 (Phase I and IIa) is now ongoing in the UK. At present, a Good Manufacturing Practice grade of PMO is produced exclusively by AVI Biopharma Inc. (http://www.avibio.com/).

Conclusions

Since the identification of dystrophin in 1987, various therapeutic approaches to DMD treatment have been evaluated, and now exon skipping, which is one of the most promising strategies, is in clinical trials. Because individual DMD patients have different mutations, exon skipping therapy requires a precise evaluation of mutations in the genome and the cDNA, and splicing patterns must be confirmed in each patient's muscle. In this point, exon skipping is a quite new, personalized therapeutic strategy. As clinicians and researchers involved in the study of muscular dystrophies, one of us for more than 50 years, we are pleased with recent progress in the field and hope that DMD patients benefit from this new therapy in the near future.

Acknowledgement

The authors thank Ms. Kumi Hoshino for typing the manuscript.

References

1) Meryon, E. (1851) On fatty degeneration of the voluntary muscles. Lancet **2**, 588–589.
2) Duchenne, G.B.A. (1868) Recherches sur la paralysie musculaire pseudo-hypertrophique, ou paralysie myo-sclerosique. Arch. Gen. Med. **11**, 3–25.
3) Monaco, A.P., Neve, R.L., Colletti-Feener, C., Bertelson, C.J., Kurnit, D.M. and Kunkel, L.M. (1986) Isolation of candidate cDNAs for portions of the Duchenne muscular dystrophy gene. Nature **323**, 646–650.
4) Hoffman, E.P., Brown, R.H. Jr. and Kunkel, L.M. (1987) Dystrophin: the protein product of the Duchenne muscular dystrophy locus. Cell **51**, 919–928.
5) Engel, A.G. and Ozawa, E. (2004) Dystrophinopathies in "Myology". 3rd ed. (eds. Engel, A.G. and Franzini-Armstrong, C.). McGraw-Hill, New York, pp. 961–1026.
6) Sibley, J.A. and Lehninger, A.L. (1949) Determination of aldolase in animal tissues. J. Biol. Chem. **177**, 859–872.
7) Sugita, H., Hattori, N. and Toyokura, Y. (1958) Determination of serum aldorase. Saishin Igaku **13**, 213–224.
8) Ebashi, S., Toyokuma, Y., Momoi, H. and Sugita, H. (1959) High creatine phosphokinase activity of sera of progressive muscular dystrophy. J. Biochem. **46**, 103–104.
9) Arahata, K., Ishiura, S., Ishiguro, T., Tsukahara, T., Suhara, Y., Eguchi, C. *et al.* (1988) Immunostaining of skeletal and cardiac muscle surface membrane with antibody against Duchenne muscular dystrophy peptide. Nature **333**, 861–863.
10) Arnett, A.L., Chamberlain, J.R. and Chamberlain, J.S. (2009) Therapy for neuromuscular disorders. Curr. Opin. Genet. Dev. **19**, 290–297.
11) Trollet, C., Athanasopoulos, T., Popplewell, L., Malerba, A. and Dickson, G. (2009) Gene therapy for muscular dystrophy: current progress and future prospects. Expert Opin. Biol. Ther. **9**, 849–866.
12) Yokota, T., Takeda, S., Lu, Q.L., Partridge, T.A., Nakamura, A. and Hoffman, E.P. (2009) A renaissance for antisense oligonucleotide drugs in neurology: exon skipping breaks new ground. Arch. Neurol. **66**, 32–38.
13) Takeshima, Y., Yagi, M., Wada, H., Ishibashi, K., Nishiyama, A., Kakumoto, M. *et al.* (2006) Intravenous infusion of an antisense oligonucleotide results in exon skipping in muscle dystrophin mRNA of Duchenne muscular dystrophy. Pediatr. Res. **59**, 690–694.
14) Nakamura, A. and Takeda, S. (2009) Exon-skipping therapy for Duchenne muscular dystrophy. Neuropathology **29**, 494–501.
15) Wu, B., Moulton, H.M., Iversen, P.L., Jiang, J., Li, J., Spurney, C.F. *et al.* (2008) Effective rescue of dystrophin improves cardiac function in dystrophin-deficient mice by a modified morpholino oligomer. Proc. Natl. Acad. Sci. USA **105**, 14814–14819.
16) Wu, B., Li, Y., Morcos, P.A., Doran, T.J., Lu, P. and Lu, Q.L. (2009) Octa-guanidine morpholino restores dystrophin expression in cardiac and skeletal muscles and ameliorates pathology in dystrophic mdx mice. Mol. Ther. **17**, 864–871.
17) Wee, K.B., Pramono, Z.A., Wang, J.L., MacDorman, K.F., Lai, P.S. and Yee, W.C. (2008) Dynamics of co-transcriptional pre-mRNA folding influences the induction of dystrophin exon skipping by antisense oligonucleotides. PLoS One **3**, e1844.
18) Aartsma-Rus, A., Janson, A.A., Kaman, W.E., Bremmer-Bout, M., den Dunnen, J.T., Baas, F. *et al.* (2003) Therapeutic antisense-induced exon skipping in cultured muscle cells from six different DMD patients. Hum. Mol. Genet. **12**, 907–914.

19) Sicinski, P., Geng, Y., Ryder-Cook, A.S., Barnard, E.A., Darlison, M.G. and Barnard, P.J. (1989) The molecular basis of muscular dystrophy in the mdx mouse: a point mutation. Science **244**, 1578–1580.
20) Lu, Q.L., Mann, C.J., Lou, F., Bou-Gharios, G., Morris, G.E., Xue, S.A. *et al.* (2003) Functional amounts of dystrophin produced by skipping the mutated exon in the mdx dystrophic mouse. Nat. Med. **9**, 1009–1014.
21) Lu, Q.L., Rabinowitz, A., Chen, Y.C., Yokota, T., Yin, H., Alter, J. *et al.* (2005) Systemic delivery of antisense oligoribonucleotide restores dystrophin expression in body-wide skeletal muscles. Proc. Natl. Acad. Sci. USA **102**, 198–203.
22) Wells, K.E., Fletcher, S., Mann, C.J., Wilton, S.D. and Wells, D.J. (2003) Enhanced in vivo delivery of antisense oligonucleotides to restore dystrophin expression in adult mdx mouse muscle. FEBS Lett. **552**, 145–149.
23) Alter, J., Lou, F., Rabinowitz, A., Yin, H., Rosenfeld, J., Wilton, S.D. *et al.* (2006) Systemic delivery of morpholino oligonucleotide restores dystrophin expression bodywide and improves dystrophic pathology. Nat. Med. **12**, 175–177.
24) Shimatsu, Y., Katagiri, K., Furuta, T., Nakura, M., Tanioka, Y., Yuasa, K. *et al.* (2003) Canine X-linked muscular dystrophy in Japan ($CXMD_J$). Exp. Anim. **52**, 93–97.
25) Urasawa, N., Wada, M.R., Machida, N., Yuasa, K., Shimatsu, Y., Wakao, Y. *et al.* (2008) Selective vacuolar degeneration in dystrophin-deficient canine Purkinje fibers despite preservation of dystrophin-associated proteins with overexpression of Dp71. Circulation **117**, 2437–2448.
26) Yokota, T., Lu, Q.L., Partridge, T., Kobayashi, M., Nakamura, A., Takeda, S. *et al.* (2009) Efficacy of systemic morpholino exon-skipping in Duchenne dystrophy dogs. Ann. Neurol. **65**, 667–676.
27) Goyenvalle, A., Vulin, A., Fougerousse, F., Leturcq, F., Kaplan, J.C., Garcia, L. *et al.* (2004) Rescue of dystrophic muscle through U7 snRNA-mediated exon skipping. Science **306**, 1796–1799.
28) Benchaouir, R., Meregalli, M., Farini, A., D'Antona, G., Belicchi, M., Goyenvalle, A. *et al.* (2007) Restoration of human dystrophin following transplantation of exon-skipping-engineered DMD patient stem cells into dystrophic mice. Cell Stem Cell **1**, 646–657.
29) Quenneville, S.P., Chapdelaine, P., Skuk, D., Paradis, M., Goulet, M., Rousseau, J. *et al.* (2007) Autologous transplantation of muscle precursor cells modified with a lentivirus for muscular dystrophy: human cells and primate models. Mol. Ther. **15**, 431–438.
30) Chaouch, S., Mouly, V., Goyenvalle, A., Vulin, A., Mamchaoui, K., Negroni, E. *et al.* (2009) Immortalized skin fibroblasts expressing conditional MyoD as a renewable and reliable source of converted human muscle cells to assess therapeutic strategies for muscular dystrophies: validation of an exon-skipping approach to restore dystrophin in Duchenne muscular dystrophy cells. Hum. Gene Ther. **20**, 784–790.
31) Wein, N., Avril, A., Bartoli, M., Beley, C., Chaouch, S., Laforet, P. *et al.* (2010) Efficient bypass of mutations in dysferlin deficient patient cells by antisense-induced exon skipping. Hum. Mutat. **31**, 136–142.
32) Nakamura, A., Yoshida, K., Fukushima, K., Ueda, H., Urasawa, N., Koyama, J. *et al.* (2008) Follow-up of three patients with a large in-frame deletion of exons 45–55 in the Duchenne muscular dystrophy (DMD) gene. J. Clin. Neurosci. **15**, 757–763.
33) Béroud, C., Tuffery-Giraud, S., Matsuo, M., Hamroun, D., Humbertclaude, V., Monnier, N. *et al.* (2007) Multiexon skipping leading to an artificial DMD protein lacking amino acids from exons 45 through 55 could rescue up to 63% of patients with Duchenne muscular dystrophy. Hum. Mutat. **28**, 196–202.
34) Araki, E., Nakamura, K., Nakao, K., Kameya, S., Kobayashi, O., Nonaka, I. *et al.* (1997) Targeted disruption of exon 52 in the mouse dystrophin gene induced muscle degeneration similar to that observed in Duchenne muscular dystrophy. Biochem. Biophys. Res. Commun. **238**, 492–497.
35) van Deutekom, J.C., Janson, A.A., Ginjaar, I.B., Frankhuizen, W.S., Aartsma-Rus, A., Bremmer-Bout, M. *et al.* (2007) Local dystrophin restoration with antisense oligonucleotide PRO051. N. Engl. J. Med. **357**, 2677–2686.
36) Kinali, M., Arechavala-Gomeza, V., Feng, L., Cirak, S., Hunt, D., Adkin, C. *et al.* (2009) Local restoration of dystrophin expression with the morpholino oligomer AVI-4658 in Duchenne muscular dystrophy: a single-blind, placebo-controlled, dose-escalation, proof-of-concept study. Lancet Neurol. **8**, 918–928.

(Received Apr. 14, 2010; accepted Jun. 3, 2010)

Profile

Hideo Sugita was born in 1930. He was graduated from Faculty of Medicine, University of Tokyo in 1954. In 1959, Prof. S. Ebashi and coworkers, including Sugita discovered the increase in serum creatine kinase (CK) in muscular dystrophy. Even now, an elevated level of serum CK is the most useful marker in the diagnosis of muscular dystrophy. Since then, he had been concentrated his efforts to elucidate the pathogenesis of muscular dystrophy. In 1988, his research group at the National Institute of Neuroscience, National Center of Neurology and Psychiatry (NCNP) clarified that dystrophin, the gene product of Duchenne muscular dystrophy (DMD) was located along the surface membrane of the skeletal and cardiac muscles and absent in DMD muscles. He was promoted to Director General of the Institute in 1989 and devoted himself to the progress of neuroscience research, health and welfare of the patients suffering from mental, neurological and developmental disorders. He was awarded Uehara Prize in 1986 and The Takeda Prize for Medical Science in 1996. He was installed as the President of NCNP in 1994 and retired in 1998. Since 2009, he is the President of Japan Foundation for Neuroscience and Mental Health.

OPEN ACCESS Freely available online

PLoS one

Antisense PMO Found in Dystrophic Dog Model Was Effective in Cells from Exon 7-Deleted DMD Patient

Takashi Saito[1,2], Akinori Nakamura[1], Yoshitsugu Aoki[1], Toshifumi Yokota[3], Takashi Okada[1], Makiko Osawa[2], Shin'ichi Takeda[1]*

1 Department of Molecular Therapy, National Institute of Neuroscience, National Center of Neurology and Psychiatry, Kodaira, Tokyo, Japan, **2** Department of Pediatrics, School of Medicine, Tokyo Women's Medical University, Shinjuku, Tokyo, Japan, **3** Research Center for Genetic Medicine, Children's National Medical Center, Washington, District of Columbia, United States of America

Abstract

Background: Antisense oligonucleotide-induced exon skipping is a promising approach for treatment of Duchenne muscular dystrophy (DMD). We have systemically administered an antisense phosphorodiamidate morpholino oligomer (PMO) targeting dystrophin exons 6 and 8 to a dog with canine X-linked muscular dystrophy in Japan ($CXMD_J$) lacking exon 7 and achieved recovery of dystrophin in skeletal muscle. To date, however, antisense chemical compounds used in DMD animal models have not been directly applied to a DMD patient having the same type of exon deletion. We recently identified a DMD patient with an exon 7 deletion and tried direct translation of the antisense PMO used in dog models to the DMD patient's cells.

Methodology/Principal Findings: We converted fibroblasts of $CXMD_J$ and the DMD patient to myotubes by FACS-aided MyoD transduction. Antisense PMOs targeting identical regions of dog and human dystrophin exons 6 and 8 were designed. These antisense PMOs were mixed and administered as a cocktail to either dog or human cells *in vitro*. In the $CXMD_J$ and human DMD cells, we observed a similar efficacy of skipping of exons 6 and 8 and a similar extent of dystrophin protein recovery. The accompanying skipping of exon 9, which did not alter the reading frame, was different between cells of these two species.

Conclusion/Significance: Antisense PMOs, the effectiveness of which has been demonstrated in a dog model, achieved multi-exon skipping of dystrophin gene on the FACS-aided MyoD-transduced fibroblasts from an exon 7-deleted DMD patient, suggesting the feasibility of systemic multi-exon skipping in humans.

Citation: Saito T, Nakamura A, Aoki Y, Yokota T, Okada T, et al. (2010) Antisense PMO Found in Dystrophic Dog Model Was Effective in Cells from Exon 7-Deleted DMD Patient. PLoS ONE 5(8): e12239. doi:10.1371/journal.pone.0012239

Editor: Antoni L. Andreu, Hospital Vall d'Hebron, Spain

Received May 7, 2010; **Accepted** July 21, 2010; **Published** August 18, 2010

Funding: This work was supported by the Health and Labour Sciences Research Grants for Translational Research from the Ministry of Health, Labour and Welfare of Japan (H19-Translational Research-003, H21-Translational Research-011, H21-Clinical Research-011). The funders had no role in study design, data collection and analysis, decision to publish, or preparation of the manuscript.

Competing Interests: The authors have declared that no competing interests exist.

* E-mail: takeda@ncnp.go.jp

Introduction

Antisense oligonucleotides (AON) have been reported to modulate splicing of pre-mRNA transcribed from mutated genes and to restore a normal reading frame in several diseases. Duchenne muscular dystrophy (DMD), a degenerative muscle disorder caused mainly by nonsense or frame-shift mutations of the dystrophin gene, is one of the diseases that could be treated by AON-mediated exon skipping. Previously reported studies were conducted *in vitro*, in animal models, and as patient intervention studies, and they showed restorations of the reading frame in dystrophin mRNA and recoveries of dystrophin protein expression [1,2,3]. Among the several AON chemistries that have been introduced thus far, a phosphorodiamidate morpholino oligomer (PMO) and 2'-O-methyl phosphorothioate (2'OMe) oligomer are promising candidates owing to their stabilities and efficacies, and they are now undergoing phase I-II clinical trials in the United Kingdom and the Netherlands, respectively [4,5]. The AON-mediated exon skipping is already in a late early stage of clinical application; therefore, it is rational to translate pre-clinical animal model knowledge into a patient-based study.

We have previously reported that the systemic administration of an antisense PMO for canine X-linked muscular dystrophy in Japan ($CXMD_J$) achieved restoration of dystrophin and amelioration of symptoms [6]. $CXMD_J$ harbors a splice site mutation within the splice acceptor site of intron 6 of the dystrophin gene. The mutation disrupts the splicing of exon 7, and thus the dystrophin mRNA lacks exon 7 [7]. In $CXMD_J$, multiple skipping of exons 6 and 8 restores the reading frame, and the multi-exon skipping approach is expected to expand the number of DMD cases potentially treatable by exon skipping [8]. $CXMD_J$ is an ideal model of multi-exon skipping, and we hope to translate the results to human patients. However, in the road to ongoing clinical trials, *in vitro* assays on patient cells are indispensable.

To date, antisense sequences used for exon skipping in DMD animal models have not been directly applied to a DMD patient having the same type of exon deletion. We identified an exon 7-deleted patient (referred to as DMD 8772) and tried direct

translation of the antisense PMO design from a DMD dog model to the DMD patient. We tried *in vitro* multi-exon skipping with the same antisense PMO that was used in $CXMD_J$ in the patient's cells before attempting delivery of the PMO into the patient.

Which cells should be used for *in vitro* dystrophin exon skipping is controversial. Myoblasts are usually employed simply because they express enough dystrophin as mRNA and protein, but collecting them requires an invasive muscle biopsy. In cases where myoblasts were not available, it had been reported that the dystrophin mRNA was detected in lymphocytes and fibroblasts by nested RT-PCR. Some studies actually demonstrated the success of exon skipping in mRNA of lymphoblastoid cells and fibroblasts [9,10], but the restoration of dystrophin protein could not be analyzed in these cells because their transcripts were illegitimate and too low to be translated into gene products [11]. As another alternative, fibroblasts are converted to myotubes by MyoD transduction [4,12,13]. Transduced cells express dystrophin mRNA and protein, but achievement of sufficient protein expression is challenging [14,15,16]. In this study, we addressed this issue by introducing a retroviral vector co-expressing MyoD and green fluorescent protein (GFP) and flow cytometry, and then quantified the dystrophin expression of the cells to evaluate the feasibility of exon skipping.

We first report multiple skipping of dystrophin exons 6 and 8 in the DMD patient's cells and translation of the unified antisense PMO design from a DMD dog model to a human based on the MyoD-transduction method utilizing flow cytometry.

Results

Mutation analysis of DMD 8772

DMD 8772, a 22-year-old man, manifested severe muscle weakness, wheelchair dependency, and mild cardiac dysfunction. No evidence of dystrophin protein had been observed on a previous muscle biopsy, and the patient had been diagnosed with a frame-shift deletion of dystrophin exon 7 by multiplex ligation-dependent probe amplification (MLPA) analysis. The deletion of exon 7 leads to a premature translation termination at exon 8. The deletion of exon 9 is known as a common splice variant maintaining the reading frame in dogs and humans [17,18] (**Figure 1A**). RT-PCR analysis of dystrophin mRNA using the patient's lymphocytes showed an exon 7 deletion, and direct sequence analysis of the RT-PCR products revealed a conjunction of exons 6 and 8 (**Figure 1B**). To determine the intron length, we performed a deletion breakpoint analysis. The genomic PCR roughly narrowed the breakpoint window to 2.5 kb between introns 6 and 7, then primer walking sequence analysis revealed the 50.4 kb deletion (Vega v35 chromosome X 32771568 to 32821979) [13] and the breakpoint accompanying an insertion of 13 bases of unknown origin (**Figure 1C**).

Myogenic conversion of fibroblasts by MyoD transduction and selection of appropriate cell lineage for exon skipping

We prepared lymphoblastoid cells, fibroblasts, and MyoD-transduced fibroblasts from DMD 8772 and assessed the feasibility of exon skipping in these cells. To establish MyoD-transduced fibroblasts, primary fibroblasts were transfected by a retrovirus encoding murine or human MyoD and GFP with the vesicular stomatitis virus (VSV-G) envelope through standard procedures (**Figure 2A**) [19,20]. To compare exon skipping between corresponding cells of $CXMD_J$ and DMD 8772, fibroblasts from both were converted. In addition, normal dog and human fibroblasts were also transduced for evaluation. After virus transfection, we

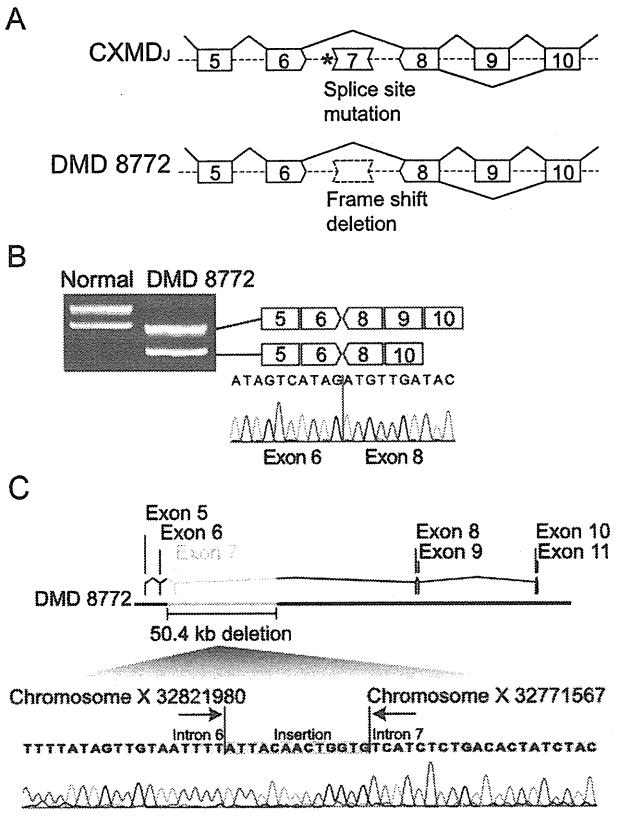

Figure 1. Mutation analysis of DMD 8772. (A) Splice-site mutation of a splice acceptor site in intron 6 (asterisk) excludes exon 7 from dog dystrophin mRNA. Frame-shift deletion of dystrophin exon 7 in DMD 8772 was diagnosed by MLPA analysis. Skipping of exon 9 is a frequent splice variant. Both ends of the schematic box of the exon represent a phase of the codon (see detail, Yokota et al. 2009). (B) RT-PCR and sequence analysis of dystrophin mRNA using normal and DMD 8772 lymphocytes. Double bands due to a splicing variant of exon 9 were observed. (C) Breakpoint analysis of DMD 8772 revealed a 50.4 kb deletion from intron 6 to intron 7, and the insertion of 13 bases of unknown origin.
doi:10.1371/journal.pone.0012239.g001

sorted GFP-positive cells by flow cytometry. The ratio of GFP-positive to -negative cells was dependent on cell lineage, and affected cells generally showed lower transfection efficiencies (**Figure 2B**). The GFP-positive cells were isolated in serum-deprived medium for myogenic differentiation and cultured for 10 to 16 days. We confirmed that the cultured cells had the morphological features of myotubes of multiple nuclei and longitudinal growth. Immunostaining analysis showed nuclear localization of MyoD and expressions of the muscle-specific proteins desmin, myosin heavy chain, and dystrophin (**Figure 2C**). Using normal dog and human fibroblasts, we performed time-course expression analyses of dystrophin mRNA by qRT-PCR and dystrophin protein by Western blot. The results showed a gradual increase in dystrophin expression. In dog cells, dystrophin became detectable on the protein level seven days after differentiation, whereas human cells required two weeks or more (**Figure 2D**). We compared the dystrophin mRNA expression of the lymphoblastoid cells, fibroblasts, and MyoD-transduced fibroblasts from DMD 8772. The MyoD-transduced fibroblasts showed remarkable expression compared with the other cells (**Figure 2E**). We tried exon skipping in lymphoblastoid cells, fibroblasts and MyoD-transduced fibroblasts, but only the MyoD-transduced

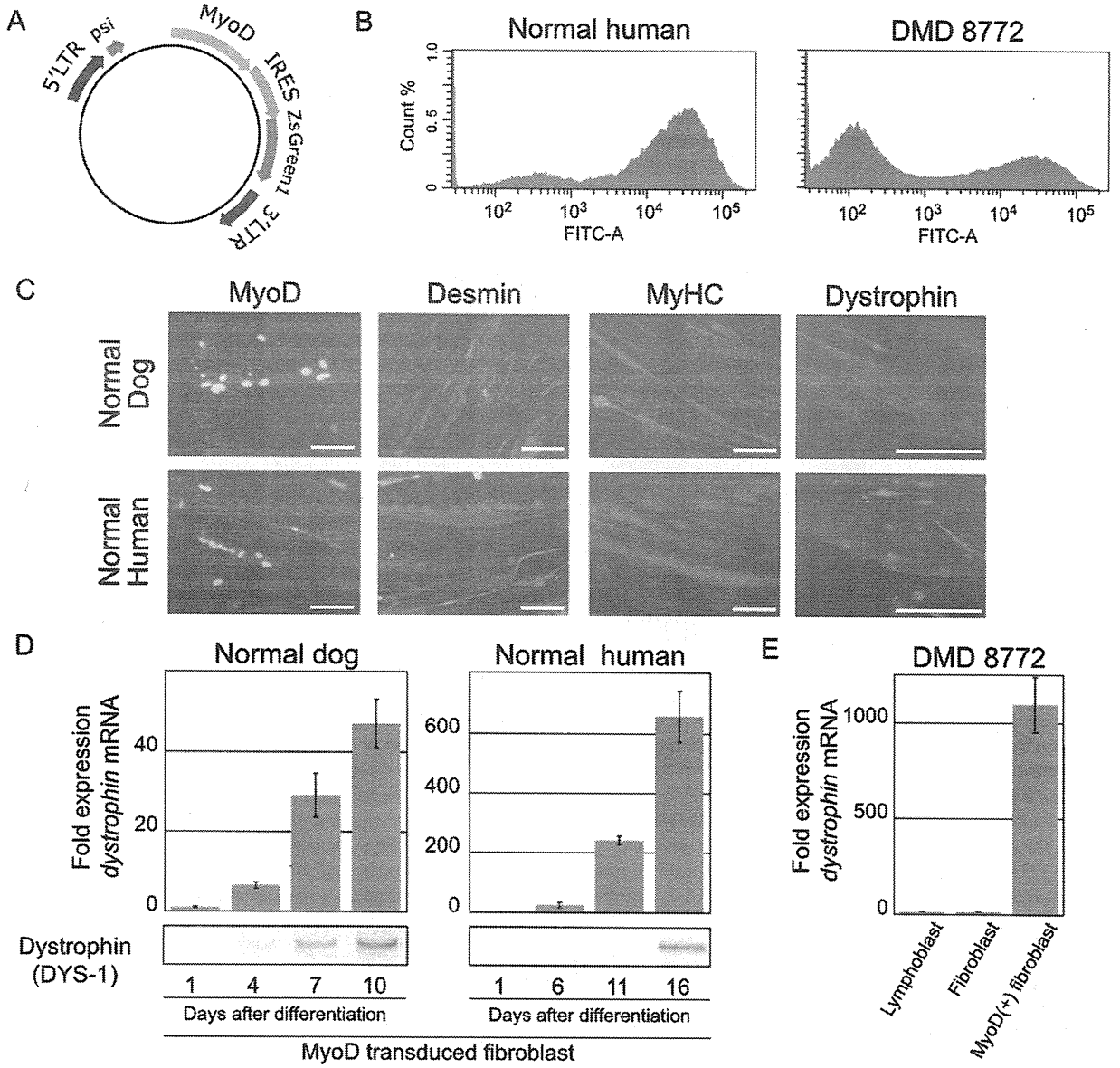

Figure 2. Myogenic conversion of fibroblasts and dystrophin expression. (A) Schematic diagram of the retroviral expression vector. (B) Histograms showing GFP fluorescence intensity compared with cell numbers of normal human and DMD 8772 MyoD-GFP-transduced fibroblasts. Both cells were analyzed five days after retroviral transfection. (C) Immunostaining of MyoD-transduced of dog and human fibroblasts after 10 and 15 days of myogenic differentiation, respectively. MyHC, myosin heavy chain. The nuclei were counter-stained with DAPI. Scale bar: 100 μm. (D) The time course of dystrophin expression in dog and human MyoD-transduced fibroblasts by qRT-PCR and immunoblotting analysis. The mRNA levels were normalized to *GAPDH* and expressed relative to the amount of the lowest one in each group. For immunoblotting, 5 μg of total protein was loaded into each lane. Error bars indicate standard deviation. (E) Determination of dystrophin mRNA expression in each cell type from DMD 8772 by qRT-PCR. MyoD-transduced fibroblasts were assayed 15 days after differentiation. Normalization and relative expression are the same as (D).
doi:10.1371/journal.pone.0012239.g002

fibroblasts yielded reproducible results. The lymphoblastoid cells and fibroblasts often failed to produce PCR products, and the skipped in-frame products were undetectable even if PCR products were generated (**data not shown**). Therefore, we used MyoD-transduced fibroblasts in the subsequent assays.

Antisense PMO sequence design

In a previous systemic dog study, we used three antisense sequences, Ex6A, Ex6B, and Ex8A, as three antisense PMO cocktails [6]. Because there were two base mismatches between dog and human Ex6B, hEx6B was newly designed on the identical region of Ex6B, modifying the mismatches of the human sequence. In the systemic study, we skipped exon 6 with a combination of Ex6A and Ex6B, and thus we tried same strategy for exon 8. We newly designed several antisense PMOs targeting exon 8 that were positioned on the identical sequence in dog and human considering the predicted *in silico* splice-enhancer motifs (**Figure 3A**). A preliminary assay of $CXMD_J$ cells showed that three sequences, Ex8G, Ex8I, and Ex8K, were effective. Therefore, the antisense combination for exon 8 contained an extra antisense sequence

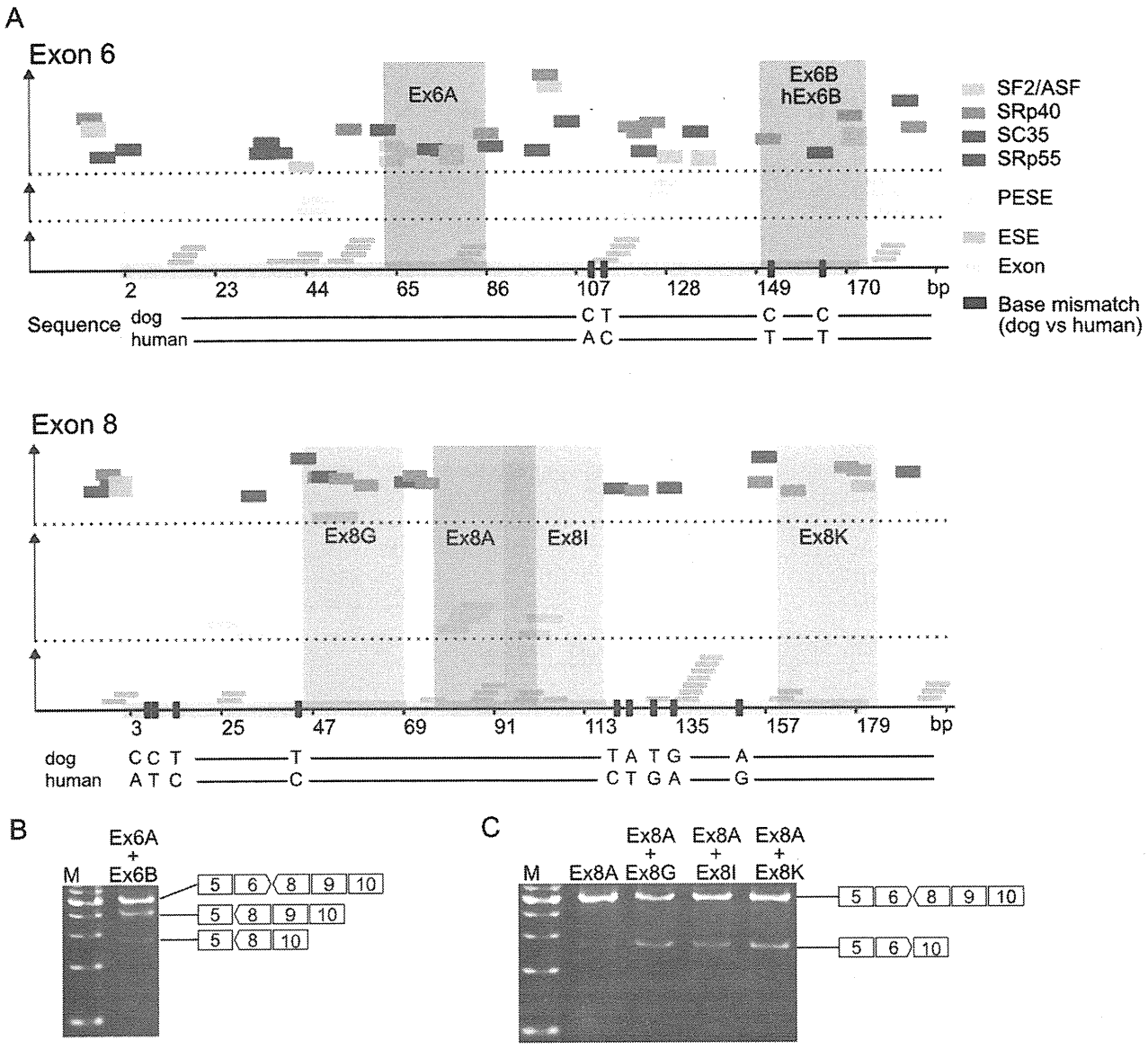

Figure 3. Design of antisense PMO sequence targeting exons 6 and 8. (A) Exonic splicing enhancer motifs predicted *in silico* based on human sequence (small coloured boxes) and positions of antisense PMOs (green and blue rectangular areas). The horizontal axis represents base positions in each exon from 5′ to 3′, and the vertical axis represents relative predicted values of the motifs. PESE: putative exonic splicing enhancer. ESE: exonic splicing enhancer. Base mismatches between dog and human (black bar) are indicated in the exon (grey box). RT-PCR of dystrophin mRNA of MyoD-transduced CXMD$_J$ fibroblasts treated with (B) a mixture of Ex6A and Ex6B and (C) only Ex8A or mixtures containing Ex8A.
doi:10.1371/journal.pone.0012239.g003

from Ex8G, Ex8I, or Ex8K in addition to that of Ex8A. The skipping efficacy of each combination was higher than that of Ex8A alone, and those of Ex8G, Ex8I, and Ex8K were comparable (**Figure 3C**).

Comparison of multiple skipping of exons 6 and 8 between CXMD$_J$ and DMD 8772 cells

The multi-exon skipping of exons 6 and 8 employed three- and four-antisense PMO cocktails. In the three-antisense PMO cocktail for dogs, Ex6A, Ex6B, and Ex8A were included, and Ex6B was replaced with hEx6B for the human. The four-antisense PMO cocktail included one of Ex8G, Ex8I, or Ex8K in addition to the three-antisense PMO cocktail (**Figure 4A**). When we transfected the three- or four-antisense PMO cocktails into the MyoD-transduced fibroblasts, we did not observe the skipped products (231 bp) of exons 6-8 on RT-PCR analyses of CXMD$_J$ but did observe the skipped products (99 bp) of exons 6-9. A sequence analysis also confirmed the concatenation of exons 5 and 10. In DMD 8772, we observed skipped products (221 bp and 92 bp, respectively) of both exons 6-8 and exons 6-9. Sequence analysis also showed that the skipped products were concatenations of exons 5 to 9 and exons 5 to 10. The four-PMO cocktails produced more in-frame products than the three-PMO cocktail, but we discerned no difference among the four PMO cocktails. This tendency was also consistent between CXMD$_J$ and DMD 8772 (**Figure 4B**). Immunostaining analysis showed partial recovery of dystrophin in the four-antisense PMO

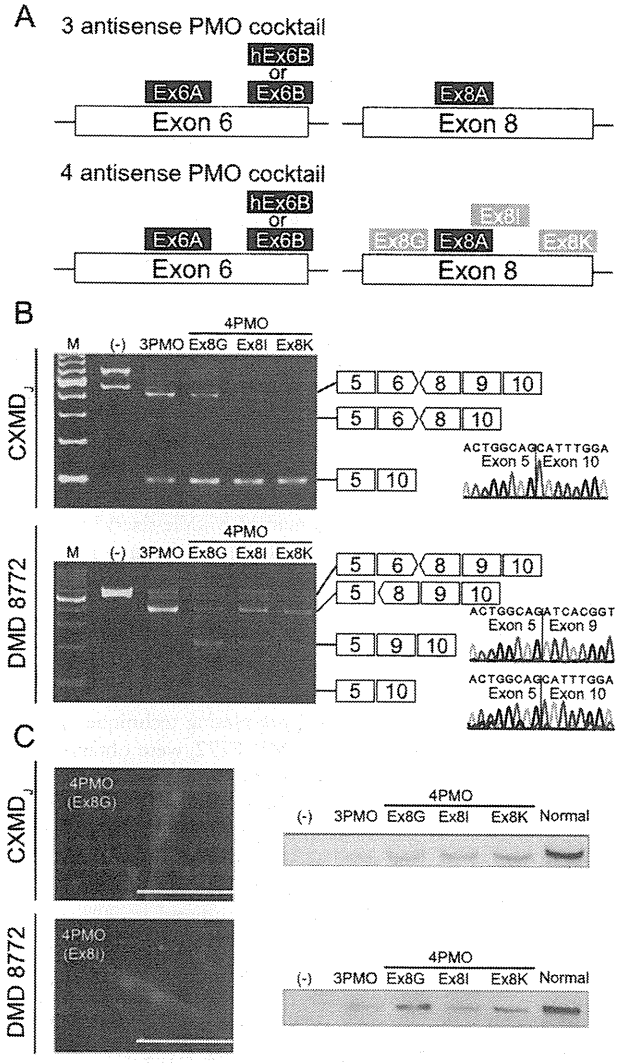

Figure 4. Multi exon skipping and recovery of dystrophin in CXMD$_J$ and DMD 8772-derived cells. (A) Schematic diagram of the three- and four-antisense PMO cocktails. For DMD 8772, Ex6B was replaced with hEx6B. In the four-antisense PMO cocktail, one additional sequence (Ex8G, Ex8I, or Ex8K) was added to the three-antisense PMO cocktail. (B) RT-PCR of dystrophin mRNA isolated from MyoD-transduced fibroblasts after treatment with the three- and four-antisense PMO cocktails. In-frame exon skipping products were 99 bp in dog and 221 bp and 92 bp in human. (C) Representative immunostaining and immunoblotting analysis of MyoD-transduced fibroblasts treated with antisense PMO cocktails. The nuclei were counterstained with DAPI. Scale bar: 100 μm. Expected molecular weights of truncated human dystrophin with exons 6–8 and exons 6–9 skipped are 18.3 kDa and 23.1 kDa, respectively, smaller than the full-length dystrophin.
doi:10.1371/journal.pone.0012239.g004

cocktail-treated cells without obvious differences between them (**Figure 4C**). Western blots of dystrophin showed products that were slightly smaller than the full-length dystrophin. In RT-PCR of DMD 8772, skipped mRNA of both exons 6-8 and 6-9 were detected; however, distinguishing the truncated dystrophins translated from these mRNA variants was impossible. Similar to the RT-PCR results, the dystrophin expression level was higher with a four-PMO cocktail than with the three-PMO cocktail. Differences between the four-PMO cocktails were also undetectable.

Discussion

In this study, we accomplished *in vitro* multi-exon skipping in a DMD patient carrying the same deletion as CXMD$_J$ by using the identical antisense PMO. We also addressed the efficient MyoD transduction of fibroblasts with FACS, and discuss the difference of the spliced exon associated with it with the frequency of alternative splicing.

FACS-aided MyoD transduction provided sufficient dystrophin expression

We evaluated the appropriateness of lymphoblastoid cells, fibroblasts, and MyoD-transduced fibroblasts as an alternative to myoblasts for exon-skipping assays. Lymphoblastoid cells and primary fibroblasts dystrophin mRNA required reamplification by nested RT-PCR [9,10], and the results were not reproducible, suggesting that low dystrophin expression may hamper reliable quantitative assessments. Only MyoD-transduced fibroblasts showed reproducible results due to their stable dystrophin expression. We employed flow cytometry for selection of MyoD-positive cells; it seems to offer several advantages against conventional drug-resistance selection. First, the transfection ratio in drug-resistance selection remains unknown until a selective drug is added. In contrast, with MyoD-transduced fibroblasts, we were able to roughly determine the ratio by fluorescence microscopy and adjust the culture scale to meet the size of the assay. Second, a low rate of myotubes formation after drug-resistance selection has been reported [21]. Our method actively selects MyoD-positive cells and enables pure clusters of MyoD-positive cells to form myotubes efficiently. MyoD transduction with GFP has been reported in several studies [22,23] but not in dystrophin exon-skipping studies. We demonstrated that it is a suitable approach for the exon-skipping assay here as well. Several studies have reported difficulties inducing dystrophin in human cells with MyoD transduction [14,15,16]. In our experience, the typical morphological features of myotubes, multiple nuclei and longitudinal cell growth, do not necessarily indicate sufficient dystrophin expression. Seeding MyoD-positive cells at high density ($>5.0\times10^4$ cells/cm^2) and incubating for longer periods (>2 weeks) were critical to induce sufficient dystrophin expression. Detachment of differentiated myotubes from culture wells was also problematic; supporting them with a coating matrix seems to promise better results.

Direct translation of antisense PMO from dog to human was feasible

We previously reported systemic multi-exon skipping in CXMD$_J$ with a 3-antisense PMO cocktail and amelioration of dystrophic pathology [6]. The effectiveness of the 3-antisense PMO cocktail was confirmed in MyoD-transduced fibroblasts derived from DMD 8772 as well. When the dog and human sequences were compared, 97% of dystrophin exon 6 and 95% of dystrophin exon 8 matched on the sequence level. This similarity enabled use of the unified antisense design methodology targeting the same sequence. We demonstrated that the identical antisense PMO sequence designed for dog and achieved multi-skipping of exons 6 and 8 in human cells. The skipping efficacies of the PMOs were indistinguishable between CXMD$_J$ and DMD 8772; the superior efficacy of the four-PMO cocktail against that of the three-PMO cocktail and the equivalent efficacies of each four-PMO cocktail were comparable. CXMD$_J$ shows more similarity in the pathogenic phenotype to human DMD than to *mdx* mice [24]. These findings imply that not only the similarity in the sequence but also the similarity in the pathogenic phenotype contributed to the comparable results.

No study has yet compared the exon skipping due to identical antisense PMOs between cells of different species carrying same exon deletion in mRNA. Recent investigations have reported a limitation in designing efficient antisenses to induce human dystrophin skipping in a mice model assay [25]; however, we confirmed the feasibility of direct translation of an antisense PMO from a DMD dog model to a DMD patient, at least *in vitro*, for the first time.

The four-antisense PMO cocktail, the addition of a fourth antisense sequence to the three-antisense PMO cocktail, increased the efficiency of skipping as previously reported [26,27]. The effectiveness of the four-antisense PMO cocktails, however, must be evaluated *in vivo*, and we are planning systemic treatment of $CXMD_J$ with them. Our results underscore the usefulness of $CXMD_J$ as a DMD model for translational research and advance the prospect that systemic treatment of the DMD patient by multi-exon skipping is possible.

Mode of exon 9 skipping might be affected by frequency of alternative splicing

With the antisense PMO targeting exons 6 and 8, exon 9 was always skipped in $CXMD_J$, although it was only partially skipped in DMD 8772. Two possibilities were considered to explain the difference: (1) the effects of the shortened introns 6 and 7 due to the deletion around exon 7 in DMD 8772 (**Figure 5**), and (2) the different frequencies of alternative splicing of exon 9. For the former case, we tried exon 8 skipping using a combination of Ex8A and Ex8G in normal and affected human MyoD-transduced fibroblasts, and found that the skipping of exon 8 and exons 8/9 happened simultaneously (**Figure S1**). Therefore, it is unlikely that the intron length affects the difference. In the latter case, the untreated MyoD-transduced fibroblasts from $CXMD_J$ clearly showed one normal and one alternative transcript; on the other hand, the untreated sample from DMD 8772 showed only a normal transcript, suggesting that the frequency of alternative splicing of exon 9 is an underlying factor in the difference. It was reported that an antisense oligonucleotide targeting exon 8 facilitates the skipping of exon 9 as well as exon 8 by effecting the concatenation of exons 8 and 9 in human and dog cells [28].

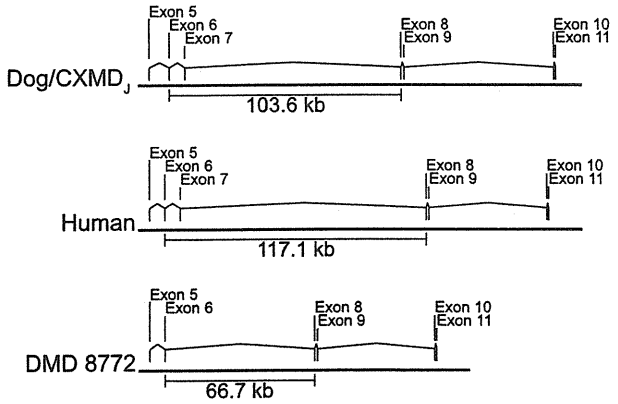

Figure 5. Location of dystrophin exons 5 to 11 in the genome. Distances from dystrophin exon 6 to exon 8 are indicated based on the GenBank reference sequences of *Canis familiaris* chromosome X genomic contig, whole genome shotgun sequence (NW_879562.1) and *Homo sapiens* 211000035840903 genomic scaffold, whole genome shotgun sequence (CH471074.1).
doi:10.1371/journal.pone.0012239.g005

These findings were observed in myoblasts but not in MyoD-tansduced fibroblasts [29,30,31]. As is well known, the mode of alternative splicing differs among various tissues [32,33], and our MyoD-transduced fibroblasts might have characteristics that are incompatible with the alternative splicing of exon 9.

In summary, MyoD transduction of fibroblasts with the help of FACS may be practical for exon skipping assays, and the direct translation of an antisense PMO from a DMD dog model to a DMD patient was feasible *in vitro*, suggesting that the animal model-based antisense PMO for multiple skipping could be effective for humans as well.

Materials and Methods

Ethics Statement

The patient samples were collected and used with the approval of the Ethics Committee of the National Center of Neurology and Psychiatry, approval ID: 20-4-6. Written informed consent was obtained from the donor. The dog study was approved by the Ethics Committee for the Treatment of Middle-sized Laboratory Animals of the National Center of Neurology and Psychiatry, approval ID: 20-05.

Cell culture

Dog primary myoblasts and fibroblasts were obtained from muscle specimens of normal and affected neonatal dogs of the $CXMD_J$ colony using a standard pre-plating technique. Primary fibroblasts of the DMD patient (DMD 8772) were obtained from skin explants and peripheral blood lymphocytes using Lymphocyte Separating Medium (PAN Biotech GmbH, Aidenbach, Germany). Lymphoblastoid cell lines were established by transformation with Epstein-Barr virus. The normal human fibroblast cell line TIG-119 was obtained from the Health Science Research Resource Bank (Osaka, Japan). Fibroblasts were cultured in 20% or 10% growth medium containing DMEM/F-12 1:1 (Invitrogen, San Diego, CA, USA), 20% or 10% fetal bovine serum, and 1% penicillin/streptomycin. For differentiation to myotubes, FACS-sorted MyoD-transduced fibroblasts were cultured in 2% differentiation medium containing DMEM/F-12 1:1, 2% horse serum, ITS Liquid Media Supplement (Sigma-Aldrich, St. Louis, MO, USA), and 1% penicillin/streptomycin.

Genomic mutation analysis

The dystrophin exon 7-deletion of DMD 8772 had been identified previously by MLPA. For breakpoint detection, lymphocyte genomic DNA was used as a template. Seven pairs of intron-spanning primers, positioned in the intron 6/7, were designed to yield 150-600 bp PCR products. A failure of PCR indicated deletions spanning the primer annealing sites. Four of seven primer pairs showed no amplification, suggesting that the deletion was more than 3.5 kb and less than 64.4 kb. Additionally, two intron 6 sense-primers and eight intron 7 antisense-primers were designed. Each primer pair was placed by flanking the breakpoint and expected to yield PCR products within the range of 4–64 kb. Primer sequences are available on request. PCR was performed using Phusion Hot Start High-Fidelity DNA Polymerase (Finnzymes, Keilaranta, Finland), and the cycling program was set to yield 16 kb products with a program of 35 cycles of 98°C for 10 sec, 60°C for 30 sec, and 72°C for 450 sec. Failure of PCR indicated products of more than 16 kb in size or the deletion of annealing sites. The breakpoint region was thus narrowed down to 2.5 kb, then primer walk sequencing was performed (Operon Biotechnologies, Tokyo, Japan).

MyoD transduction and cell sorting by FACS

The coding sequences of mouse *Myod1* (CCDS 21277.1) and human *MYOD1* (CCDS 7826.1) were derived from the Consensus CDS database [34]. The sequences were synthesized and cloned into a pUC57 vector (GenScript, Piscataway, NJ, USA). We subcloned it into a pRetroX-IRES-ZsGreen1 expression vector (Clontech, Mountain View, CA, USA). The expression vector, a pVSV-G envelope vector, and a gap-pol expression vector were co-transfected into a 293T packaging cell line using the standard calcium phosphate method. After 48–72 h incubation, the viral supernatant was collected and stored at −80°C. For retroviral transduction, the fibroblasts were harvested at 70–80% confluence in a T225 flask, and 2.5 ml thawed retroviral stock was added to 35 ml of growth medium. We added polybrene (Sigma-Aldrich) to a final concentration of 8 μg/ml. After 48–72 h incubation at 32°C, the culture medium was replaced with fresh growth medium, the cells were incubated at 37°C 1–3 d more, until the GFP-positive cells exceeded approximately 60%. Cell sorting was performed on a FACS VantageSE or FACSAria flow cytometry system (BD Bioscience, Franklin Lakes, NJ, USA). The recovered GFP-positive cells were seeded in Matrigel (BD Bioscience)-coated well plates at density of 5×10^4 cell/cm^2. After confirmation of cell attachment, the culture medium was changed to 2% differentiation medium. We cultured MyoD-transduced fibroblasts for 10 to 16 d to differentiate to myotubes.

Antisense PMO design and transfection to cultured cells

The antisense PMO sequences Ex6A, Ex6B, and Ex8A were described in Yokota et al. [6]. In addition, extra sequences hEx6B, Ex8G, Ex8I, and Ex8K were designed and synthesized (Gene Tools, LLC, Philomath, OR, USA). We used the Human Splicing Finder for *in silico* prediction of the splice-enhancer motifs [35]. All sequences are shown in **Table S1**. We transfected the antisense PMOs into myotubes differentiated from MyoD-transduced fibroblasts with a transfection agent, Endo-Porter (Gene Tools). In the 2% differentiation medium, the final concentration of the antisense PMO was 10 μM for a single sequence, 20 μM for two sequences, and a total of 30 μM for three or four sequences. A final concentration of Endo-Porter was 6 μM. After 48–72 h incubation with the PMO, the medium was changed to a fresh culture medium free of PMOs. The cells were recovered for analysis after 24–48 h in the PMO-deprived medium to allow sufficient time to translate dystrophin protein.

Quantitative RT-PCR analysis

Total RNA was extracted from MyoD-transduced fibroblasts obtained from normal subjects using Trizol (Invitrogen) at the time points specified. Total RNA (100-200 ng) was employed for cDNA synthesis using a QuantiTect Reverse Transcription Kit (Qiagen, Hilden, Germany). Quantitative real-time PCR was performed using ExTaq II SYBR (Takara, Kyoto, Japan) and a MyiQ Single-Color Real-Time PCR detection system (Bio-Rad, Hercules, CA). Primer sequences are shown in **Table S2**. Expression of dystrophin mRNA was normalized to *GAPDH* mRNA, and the time course of the increment was calculated by the delta-delta-Ct method.

RT-PCR and sequence analysis

As well as quantitative RT-PCR analysis, total RNA extraction and cDNA synthesis were performed. For myoblasts and MyoD-transduced fibroblasts, 35 cycles of denaturing at 98°C for 10 sec, annealing at 63°C for 30 sec, and extension at 72°C for 1 min were performed with ExTaq DNA polymerase (Takara). For fibroblasts and lymphoblasts, nested PCR was performed. Primer sequences are shown in **Table S3**. PCR products were electrophoresed on 1.2% SeaKem LE agarose gel (Lonza, Basel, Switzerland). The bands of interests were excised using a Wizard SV Gel and PCR Clean-Up system (Promega, Fitchburg, WI, USA), then sequenced directly or cloned into a vector using a TOPO-TA Cloning Kit (Invitrogen) with standard cloning techniques. Sequencing was performed by Fasmac Corporation (Kanagawa, Japan).

Immunostaining analysis

Cells were fixed in 3% paraformaldehyde, permeabilized in 10% Triton-X, then blocked by 10% goat serum in PBS for 1 h at room temperature. The cells were incubated with the primary antibody for 1 h at room temperature using anti-dystrophin (NCL-Dys1, diluted 1:30, Novocastra, Newcastle upon Tyne, UK), anti-myosin heavy chain (NCL-MHCf, diluted 1:30, Novocastra), anti-MyoD (NCL-MyoD1, diluted 1:30, Novocastra), or anti-desmin (NCL-DES-DERII, diluted 1:30, Novocastra). Incubation with the secondary antibody was performed for 30 min at room temperature using anti-rabbit or anti-mouse IgG (Alexa Fluor 546 highly cross-adsorbed, diluted 1:300, Invitrogen). Antibodies were diluted in Can Get Signal Immunostain A solution (Toyobo, Osaka, Japan). To visualize nuclei and enhance fluorescence signals, cells were mounted with Pro Long Gold Antifade reagent (Invitrogen).

Immunoblotting analysis

Protein was extracted from cultured cells using RIPA buffer (Thermo Fisher Scientific, Rockford, IL, USA) containing Complete Mini (Roche Applied Science, Indianapolis, IN, USA) as a protease inhibitor. Protein concentrations were determined using a BCA protein assay kit (Thermo Fisher Scientific) and equalized. After being mixed with an equal volume of EzApply sample buffer (ATTO Corporation, Tokyo, Japan), cell lysates containing equal amounts of total protein were denatured at 95°C for 5 min, electrophoresed in NuPAGE Novex Tris-Acetate Gel 3–8% (Invitrogen) at 150 V for 75 min, and transferred onto an Immobilon-P membrane (Millipore Corp., Billerica, MA, USA). Membranes were blocked for 1 h with 5% ECL Blocking agent (GE Healthcare, Buckinghamshire, UK) and probed with anti-dystrophin antibody (NCL-Dys1, diluted 1:50, Novocastra), followed by incubation with peroxidase-conjugated goat-anti-mouse IgG (Bio-Rad). An ECL Plus Western blotting system (GE Healthcare) was used to detect protein bands.

Supporting Information

Figure S1 RT-PCR of dystrophin mRNA isolated from the normal and affected human MyoD-transduced fibroblasts after the single exon 8 skipping.
Found at: doi:10.1371/journal.pone.0012239.s001 (0.30 MB PDF)

Table S1 Sequences of antisense PMO for dystrophin gene (for dog and human if not specified).
Found at: doi:10.1371/journal.pone.0012239.s002 (0.07 MB PDF)

Table S2 Sequences of qRT-PCR primers.
Found at: doi:10.1371/journal.pone.0012239.s003 (0.07 MB PDF)

Table S3 Sequences of RT-PCR primers.
Found at: doi:10.1371/journal.pone.0012239.s004 (0.07 MB PDF)

Acknowledgments

The authors thank Yu-ichi Goto (Department of Mental Retardation and Birth Defect Research, National Center of Neurology and Psychiatry), Narihiro Minami (Department of Neuromuscular Research, National Center of Neurology and Psychiatry), Hirofumi Komaki (Department of Child Neurology, National Center of Neurology and Psychiatry), Katsutoshi Yuasa (Research Institute of Pharmaceutical Sciences, Faculty of Pharmacy, Musashino University, Tokyo, Japan), and Tetsuya Nagata, Yuko Shimizu, and Satoru Masuda (Department of Molecular Therapy, National Center of Neurology and Psychiatry) for useful discussions and technical assistance.

Author Contributions

Conceived and designed the experiments: TS AN ST. Performed the experiments: TS YA. Analyzed the data: TS MO. Contributed reagents/materials/analysis tools: TY TO. Wrote the paper: TS AN ST.

References

1. Aartsma-Rus A, Bremmer-Bout M, Janson AA, den Dunnen JT, van Ommen GJ, et al. (2002) Targeted exon skipping as a potential gene correction therapy for Duchenne muscular dystrophy. Neuromuscul Disord 12(Suppl 1): S71–77.
2. Mann C, Honeyman K, Cheng A, Ly T, Lloyd F, et al. (2001) Antisense-induced exon skipping and synthesis of dystrophin in the mdx mouse. Proc Natl Acad Sci U S A 98: 42–47.
3. Alter J, Lou F, Rabinowitz A, Yin H, Rosenfeld J, et al. (2006) Systemic delivery of morpholino oligonucleotide restores dystrophin expression bodywide and improves dystrophic pathology. Nat Med 12: 175–177.
4. van Deutekom J, Janson A, Ginjaar I, Frankhuizen W, Aartsma-Rus A, et al. (2007) Local dystrophin restoration with antisense oligonucleotide PRO051. N Engl J Med 357: 2677–2686.
5. Kinali M, Arechavala-Gomeza V, Feng L, Cirak S, Hunt D, et al. (2009) Local restoration of dystrophin expression with the morpholino oligomer AVI-4658 in Duchenne muscular dystrophy: a single-blind, placebo-controlled, dose-escalation, proof-of-concept study. Lancet Neurol 8: 918–928.
6. Yokota T, Lu Q, Partridge T, Kobayashi M, Nakamura A, et al. (2009) Efficacy of systemic morpholino exon-skipping in Duchenne dystrophy dogs. Ann Neurol 65: 667–676.
7. Sharp N, Kornegay J, Van Camp S, Herbstreith M, Secore S, et al. (1992) An error in dystrophin mRNA processing in golden retriever muscular dystrophy, an animal homologue of Duchenne muscular dystrophy. Genomics 13: 115–121.
8. Béroud C, Tuffery-Giraud S, Matsuo M, Hamroun D, Humbertclaude V, et al. (2007) Multiexon skipping leading to an artificial DMD protein lacking amino acids from exons 45 through 55 could rescue up to 63% of patients with Duchenne muscular dystrophy. Hum Mutat 28: 196–202.
9. Wee K, Pramono Z, Wang J, MacDorman K, Lai P, et al. (2008) Dynamics of co-transcriptional pre-mRNA folding influences the induction of dystrophin exon skipping by antisense oligonucleotides. PLoS ONE 3: e1844.
10. Pramono Z, Takeshima Y, Alimsardjono H, Ishii A, Takeda S, et al. (1996) Induction of exon skipping of the dystrophin transcript in lymphoblastoid cells by transfecting an antisense oligodeoxynucleotide complementary to an exon recognition sequence. Biochem Biophys Res Commun 226: 445–449.
11. Chelly J, Gilgenkrantz H, Hugnot J, Hamard G, Lambert M, et al. (1991) Illegitimate transcription. Application to the analysis of truncated transcripts of the dystrophin gene in nonmuscle cultured cells from Duchenne and Becker patients. J Clin Invest 88: 1161–1166.
12. Aartsma-Rus A, Janson A, Kaman W, Bremmer-Bout M, den Dunnen J, et al. (2003) Therapeutic antisense-induced exon skipping in cultured muscle cells from six different DMD patients. Hum Mol Genet 12: 907–914.
13. Aartsma-Rus A, Janson A, Kaman W, Bremmer-Bout M, van Ommen G, et al. (2004) Antisense-induced multiexon skipping for Duchenne muscular dystrophy makes more sense. Am J Hum Genet 74: 83–92.
14. Gonçalves M, Swildens J, Holkers M, Narain A, van Nierop G, et al. (2008) Genetic complementation of human muscle cells via directed stem cell fusion. Mol Ther 16: 741–748.
15. Cooper S, Kizana E, Yates J, Lo H, Yang N, et al. (2007) Dystrophinopathy carrier determination and detection of protein deficiencies in muscular dystrophy using lentiviral MyoD-forced myogenesis. Neuromuscul Disord 17: 276–284.
16. Zheng J, Wang Y, Karandikar A, Wang Q, Gai H, et al. (2006) Skeletal myogenesis by human embryonic stem cells. Cell Res 16: 713–722.
17. McClorey G, Moulton H, Iversen P, Fletcher S, Wilton S (2006) Antisense oligonucleotide-induced exon skipping restores dystrophin expression in vitro in a canine model of DMD. Gene Ther 13: 1373–1381.
18. Reiss J, Rininsland F (1994) An explanation for the constitutive exon 9 cassette splicing of the DMD gene. Hum Mol Genet 3: 295–298.
19. Miller A, Buttimore C (1986) Redesign of retrovirus packaging cell lines to avoid recombination leading to helper virus production. Mol Cell Biol 6: 2895–2902.
20. Morgenstern J, Land H (1990) A series of mammalian expression vectors and characterisation of their expression of a reporter gene in stably and transiently transfected cells. Nucleic Acids Res 18: 1068.
21. Choi J, Costa M, Mermelstein C, Chagas C, Holtzer S, et al. (1990) MyoD converts primary dermal fibroblasts, chondroblasts, smooth muscle, and retinal pigmented epithelial cells into striated mononucleated myoblasts and multinucleated myotubes. Proc Natl Acad Sci U S A 87: 7988–7992.
22. Etzion S, Barbash I, Feinberg M, Zarin P, Miller L, et al. (2002) Cellular cardiomyoplasty of cardiac fibroblasts by adenoviral delivery of MyoD ex vivo: an unlimited source of cells for myocardial repair. Circulation 106: I125–130.
23. Noda T, Fujino T, Mie M, Kobatake E (2009) Transduction of MyoD protein into myoblasts induces myogenic differentiation without addition of protein transduction domain. Biochem Biophys Res Commun 382: 473–477.
24. Shimatsu Y, Yoshimura M, Yuasa K, Urasawa N, Tomohiro M, et al. (2005) Major clinical and histopathological characteristics of canine X-linked muscular dystrophy in Japan, CXMDJ. Acta Myol 24: 145–154.
25. Mitrpant C, Adams A, Meloni P, Muntoni F, Fletcher S, et al. (2009) Rational design of antisense oligomers to induce dystrophin exon skipping. Mol Ther 17: 1418–1426.
26. Aartsma-Rus A, Kaman W, Weij R, den Dunnen J, van Ommen G, et al. (2006) Exploring the frontiers of therapeutic exon skipping for Duchenne muscular dystrophy by double targeting within one or multiple exons. Mol Ther 14: 401–407.
27. Harding P, Fall A, Honeyman K, Fletcher S, Wilton S (2007) The influence of antisense oligonucleotide length on dystrophin exon skipping. Mol Ther 15: 157–166.
28. Aartsma-Rus A, van Ommen G (2007) Antisense-mediated exon skipping: a versatile tool with therapeutic and research applications. RNA 13: 1609–1624.
29. Wilton S, Fall A, Harding P, McClorey G, Coleman C, et al. (2007) Antisense oligonucleotide-induced exon skipping across the human dystrophin gene transcript. Mol Ther 15: 1288–1296.
30. McClorey G, Fall A, Moulton H, Iversen P, Rasko J, et al. (2006) Induced dystrophin exon skipping in human muscle explants. Neuromuscul Disord 16: 583–590.
31. Aartsma-Rus A, De Winter C, Janson A, Kaman W, Van Ommen G, et al. (2005) Functional analysis of 114 exon-internal AONs for targeted DMD exon skipping: indication for steric hindrance of SR protein binding sites. Oligonucleotides 15: 284–297.
32. Hallegger M, Llorian M, Smith C (2010) Alternative splicing: global insights. FEBS J 277: 856–866.
33. Sironi M, Cagliani R, Pozzoli U, Bardoni A, Comi G, et al. (2002) The dystrophin gene is alternatively spliced throughout its coding sequence. FEBS Lett 517: 163–166.
34. Pruitt K, Harrow J, Harte R, Wallin C, Diekhans M, et al. (2009) The consensus coding sequence (CCDS) project: Identifying a common protein-coding gene set for the human and mouse genomes. Genome Res 19: 1316–1323.
35. Desmet F, Hamroun D, Lalande M, Collod-Béroud G, Claustres M, et al. (2009) Human Splicing Finder: an online bioinformatics tool to predict splicing signals. Nucleic Acids Res 37: e67.

Efficient gene transfer into neurons in monkey brain by adeno-associated virus 8

Yoshito Masamizu[a], Takashi Okada[b], Hidetoshi Ishibashi[a], Shin'ichi Takeda[b], Shigeki Yuasa[c] and Kiyoshi Nakahara[a,d]

Although the adeno-associated virus (AAV) vector is a promising tool for gene transfer into neurons, especially for therapeutic purposes, neurotropism in primate brains is not fully elucidated for specific AAV serotypes. Here, we injected AAV serotype 8 (AAV8) vector carrying the enhanced green fluorescent protein (EGFP) gene under a ubiquitous promoter into the cerebral cortex, striatum and substantia nigra of common marmosets. Robust neuronal EGFP expression was observed at all injected sites. Cell typing with immunohistochemistry confirmed efficient AAV8-mediated gene transfer into the pyramidal neurons in the cortex, calbindin-positive medium spiny neurons in the striatum and dopaminergic neurons in the substantia nigra. The results indicate a preferential tropism of AAV8 for subsets of neurons, but not for glia, in monkey brains. *NeuroReport* **21:447–451 © 2010 Wolters Kluwer Health | Lippincott Williams & Wilkins.**

NeuroReport 2010, 21:447–451

Keywords: adeno-associated virus, gene transfer, marmoset, motor cortex, neuron, nonhuman primate, striatum, substantia nigra, tropism

[a]Department of Animal Models for Human Disease, [b]Department of Molecular Therapy, [c]Department of Ultrastructural Research, National Institute of Neuroscience, NCNP and [d]PRESTO, Japan Science and Technology Agency

Correspondence to Dr Kiyoshi Nakahara, Department of Animal Models for Human Disease, National Institute of Neuroscience, NCNP, 4-1-1 Ogawa-Higashi, Kodaira, Tokyo 187-8502, Japan
Tel: +81 42 346 1724; fax: +81 42 346 1754; e-mail: nakahara@ncnp.go.jp

Received 24 January 2010 accepted 14 February 2010

Introduction

Adeno-associated virus (AAV) vectors are promising as a means to deliver genes into a wide range of tissues *in vivo*. They are eligible as gene therapy vectors, as qualified by their nonpathogenicity and long-term gene expression, and are particularly suitable for gene transfer into neurons of the central nervous system (CNS) because of their ability to infect nondividing cells [1,2]. In addition to their therapeutic applications, AAV-mediated gene transfer into the CNS is becoming increasingly valuable in basic neurophysiological research, particularly with the advent of genetic methods for experimental manipulation of neuronal activities, such as optogenetics [3,4]. Extensive exploration of the neurotropism of AAV vectors in primate brains is thus prerequisite for application to the gene therapy of neurological disorders and to neurophysiological research.

One remarkable feature of AAV vectors is their wide variety of serotypes originating from the variation in the amino acid sequence of the capsid proteins. Infection efficiency and cell tropism of the AAV vectors are mainly determined by their serotypes, which can directly affect epitopes recognized by the host immune system and preference for the receptors used for cell entry [1]. This feature also offers researchers opportunities for selecting an appropriate AAV serotype according to their purposes and target cells. Although AAV serotype 2 (AAV2) has been the most commonly used in both clinical applications and basic research among at least 100 identified serotypes [1], recent studies have revealed the potential and advantages of other serotypes [1,5–8]. Among these, adeno-associated virus serotype 8 (AAV8) has attracted interest for its higher efficiency than AAV2 in transferring genes into CNS neurons [9]. However, neuronal tropism of AAV8 has mainly been investigated in rodent brains, and tropism of AAV8 for neuronal cell types in primate brains is not yet fully elucidated.

Here, we investigated tropism and gene transfer efficiency of AAV8 vector in the brain of a new world monkey, the common marmoset. More specifically, we explored the ability of AAV8 to deliver genes into projection neurons in the striatum and dopaminergic neurons in the substantia nigra. These neurons constitute functional circuits within the extrapyramidal system, playing pivotal roles not only in normal functions such as action selection, but also in the pathophysiology of various neurological disorders such as Parkinson's disease [10–13]. This study reveals strong neuronal tropism of AAV8, as identified by several markers for neuronal subtypes in the pyramidal and extrapyramidal systems of the primate brain.

Methods

Monkeys

Two laboratory-bred adult male common marmosets (*Callithrix jacchus*) were used. The animals were 59 months (weight, 325 g) and 62 months (weight, 358 g) of age at the start of the experiment. Animal experiments were conducted in accordance with the NIH guidelines for the care and use of laboratory animals, and with the guidelines approved by the ethics committee for primate research of the National Center of Neurology and Psychiatry, Japan.

0959-4965 © 2010 Wolters Kluwer Health | Lippincott Williams & Wilkins

DOI: 10.1097/WNR.0b013e328338ba00

Virus preparation

AAV8-enhanced green fluorescent protein (EGFP) virus production and purification was performed as described earlier [14,15]. The vector plasmid (pAAV-EGFP) contained EGFP cDNA and the woodchuck hepatitis virus post-transcriptional regulatory element (WPRE) under the control of the CAG promoter, a modified chicken β-actin promoter with a cytomegalovirus immediate early enhancer. The pAAV-EGFP vector was cotransfected with an AAV8 chimeric helper plasmid encoding the AAV2 rep gene and the AAV8 cap gene, and an adenoviral helper plasmid pAdeno [16], into HEK293 cells by calcium phosphate coprecipitation with the use of active gassing [15]. Cell suspensions were collected 72 h after transfection, and centrifuged at 300 × *g* for 10 min. Cell pellets were resuspended in 30 ml of Tris-buffered saline [100 mM Tris–HCl (pH 8.0), 150 mM NaCl]. AAV8-EGFP virus was harvested by five cycles of freeze-thawing of the resuspended pellet. The crude viral lysate was initially concentrated by a brief two-tier CsCl gradient centrifugation for 3 h [17], and further purified by dual ion-exchange chromatography [14]. The final number of AAV8-EGFP virus particles was determined by quantitative polymerase chain reaction of DNase I-treated stocks with plasmid standards, and was 3.0×10^{13} vector genomes (vg)/ml.

Virus injections

All surgical procedures and AAV8-EGFP virus injections were performed under aseptic conditions. Animals were initially anesthetized with 0.1 ml ketamine (50 mg/ml, intramuscularly). Animals were then intubated and placed in a stereotaxic apparatus with anesthesia maintained using inhaled isoflurane (1.5–2.5% in oxygen). Pulse oxygen (SpO_2), heart rate, body temperature, end-tidal CO_2 ($EtCO_2$), O_2 (EtO_2), isoflurane (EtISO), and fraction of inspired CO_2 ($FiCO_2$), O_2 (FiO_2), and isoflurane (FiISO) were continuously monitored to judge the animal's condition. After injection of 0.07 ml cefovecin (80 mg/ml, intramuscularly) as an antibiotic, a stereotaxic small craniotomy (2–3 mm in diameter) was then made over the area of interest, and the underlying dura was slit to allow penetration by the virus-containing 10-μl Hamilton syringe connected to a 33 G (45°angle) needle. Virus solution (3 μl) was injected at a rate of 0.25 μl/min to each site. Injection sites were determined using the Stereotaxic Atlas of the Marmoset Brain with Immunohistochemical Architecture and MRI Images (by Yuasa S, Nakamura K and Kohsaka S, in press). As injection sites, we aimed at the primary motor cortex: anterior (A) 12.0 mm from the interaural line, lateral (L) 6.8 mm from the midline, and ventral (V) 2.5 mm from the brain surface [18], the striatum: A 12.0 mm, L 3.0 mm, and V 6.0 mm [19], and the substantia nigra: A 5.5 mm, L 2.5 mm, and V 11.7 mm [20]. After each injection, the needle was kept in place for an additional 15 min (motor cortex) or 5 min (striatum and substantia nigra), and then slowly withdrawn (2 mm/min). We then waited 4 weeks after the virus injection for EGFP expression to appear.

Immunohistochemistry

The procedures were as reported earlier [21], with slight modifications. Briefly, 4 weeks after AAV8-EGFP virus injection, the animals were deeply anesthetized by an intraperitoneal injection of sodium pentobarbital, and then perfused through the ascending aorta with 4% paraformaldehyde dissolved in 0.1 M phosphate-buffered saline (PBS, pH 7.4). The brains were sampled, and then postfixed at 4°C for 3 days with the same fixative. The fixed brains were embedded in 3% agar in PBS, and then sliced coronally into 100 μm sections with a Microslicer (DTK-3000, DOSAKA EM, Kyoto, Japan). Immunohistochemical stainings were performed on free-floating sections. After 1 h of preincubation with 10% normal goat serum at 4°C, sections were incubated with primary antibodies in PBS containing 2% Triton X-100 at 4°C overnight. Antibodies against the following neuronal or glial marker proteins were used: neuron-specific nuclear protein (NeuN; mouse IgG, 1 : 500; Cat. No. MAB377, Millipore, Billerica, Massachusetts, USA), nonphosphorylated neurofilament protein (NNF; mouse IgG, 1 : 1000; Cat. No. SMI-32R, Sternberger Monoclonals, Baltimore, Maryland, USA) [22], calbindin D-28k (rabbit IgG, 1 : 1000; Cat. No. CB38a, Swant, Bellinzona, Switzerland), tyrosine hydroxylase (TH; mouse IgG, 1 : 1000; Cat. No. T2928, Sigma-Aldrich, St. Louis, Missouri, USA), glial fibrillary acidic protein (GFAP; rabbit IgG, 1 : 200; Cat. No. Z0334, Dako, Glostrup, Denmark), and oligodendrocyte transcription factor 2 (Olig2; rabbit IgG, 1 : 2000; Cat. No. AB9610, Millipore). Sections were then rinsed eight times with PBS, and incubated with secondary antibodies in PBS at 4°C for 5 h. Appropriate secondary antibody [Alexa goat anti-mouse 594 IgG (1 : 500; Cat. No. A11005, Molecular Probes, Eugene, Oregon, USA), or Alexa goat anti-rabbit 594 IgG (1 : 500; Cat. No. A11012, Molecular Probes)] directed against the species in which the primary antibody was raised, was used in each case. Sections were then rinsed five times with PBS. The stained sections were mounted on glass slides with Fluoromount-G (Beckman Coulter, Fullerton, California, USA) and examined with a confocal laser-scanning microscope (LSM5 Pascal, Zeiss, Oberkochen, Germany). EGFP expression was directly observed through confocal fluorescence images.

Results

Neuronal tropism of AAV8 in the marmoset brain *in vivo*

We injected recombinant AAV8 vector carrying the EGFP gene under the control of CAG promoter (AAV8-EGFP) into the brains of two common marmosets. Stereotaxic virus injections were carried out aiming at the motor cortex, the striatum and the substantia nigra. Four weeks after the injections, intense EGFP fluorescence was

directly observed in numerous cell bodies and fibers around all injected sites, indicating efficient EGFP gene transfer by the infection of AAV8-EGFP (Figs 1 and 2). As the CAG promoter has strong and ubiquitous activity, the types of EGFP-expressing ($EGFP^+$) cells would reflect endogenous tropism of AAV8 in the primate brain. Thus, we examined the tropism of AAV8-EGFP by immunostaining for neuronal or glial marker proteins. Confocal microscopic observations revealed that almost all of the $EGFP^+$ cells in the striatum were colocalized with NeuN (Fig. 1a–c). In contrast, the $EGFP^+$ cells were rarely colocalized with GFAP, or with Olig2, marker proteins for astrocytes and oligodendrocytes, respectively (Fig. 1d–i). These results indicated tropism of AAV8 for neurons, but not for glia, in the primate brain.

Identification of AAV8-infected neuronal cell types

We further characterized the $EGFP^+$ neurons by immunostaining for several markers of neuronal subtypes. In the motor cortex, most of the $EGFP^+$ cells were pyramidal neurons, as revealed by the coexpression of NNF, a cytoskeletal protein found in a subset of pyramidal neurons (Fig. 2a–d). Overlaps of EGFP fluorescence and NNF expression were evident in the apical dendrites (Fig. 2d). In the striatum, the $EGFP^+$ cells exhibited morphology characteristic of medium spiny neurons, the principal cell type in this region. Indeed, immunostaining confirmed that the majority of the $EGFP^+$ cells coexpressed calbindin, a specific marker for the medium spiny neuron [23] (Fig. 2e–h). We also found colocalization of EGFP fluorescence and TH immunoreactivity, a specific marker for dopaminergic neurons, in the substantia nigra (Fig. 2i–l).

Quantification of AAV8 infection efficiency in the identified neuronal cell types

Finally, to quantify the neuronal tropism of AAV8, we counted colocalizations of EGFP fluorescence and immunohistochemical staining of neuronal or glial marker proteins in the three injected regions ($n = 2$, Table 1). The majority of the $EGFP^+$ cells were colocalized with neuronal marker proteins, and the estimated percentages of colocalization were extremely high: 91% of the $EGFP^+$ cells colocalized with NNF in the motor cortex, 70% with calbindin in the striatum, and 99% with TH in the substantia nigra pars compacta. In the striatum, we also counted colocalizations of EGFP signal with NeuN, and the estimated percentage of colocalization reached 98%. In contrast, we hardly detected colocalization of the $EGFP^+$ cells with GFAP or with Olig2 in the three brain regions examined (3% or below).

Discussion

In this study, we injected AAV8-EGFP into three brain regions, the motor cortex, the striatum and the substantia nigra of two common marmosets. Almost all of the

Fig. 1

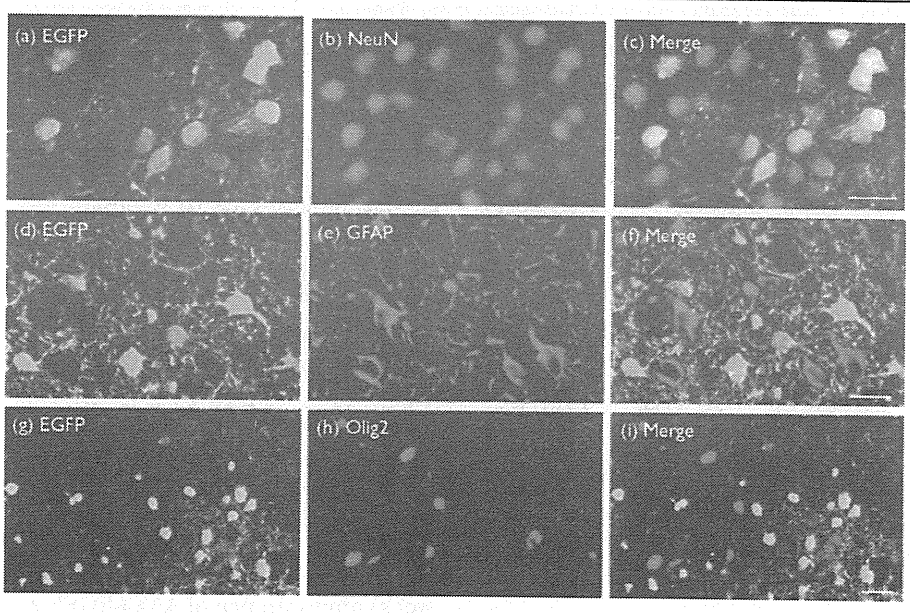

Adeno-associated virus serotype 8 preferentially transfers the enhanced green fluorescent protein (EGFP) gene into neurons in the primate striatum *in vivo*. Confocal images show EGFP-positive ($EGFP^+$) cells in the striatum (a, d, g; green). $EGFP^+$ cells are colocalized with neuron-specific nuclear protein (NeuN, b; red) as shown by the merged image (c; yellow). $EGFP^+$ cells are rarely colocalized with glial fibrillary acidic protein (GFAP, e; red) or oligodendrocyte transcription factor 2 (Olig2, h; red) as shown by the merged images (f and i). Bars: 20 μm.

Fig. 2

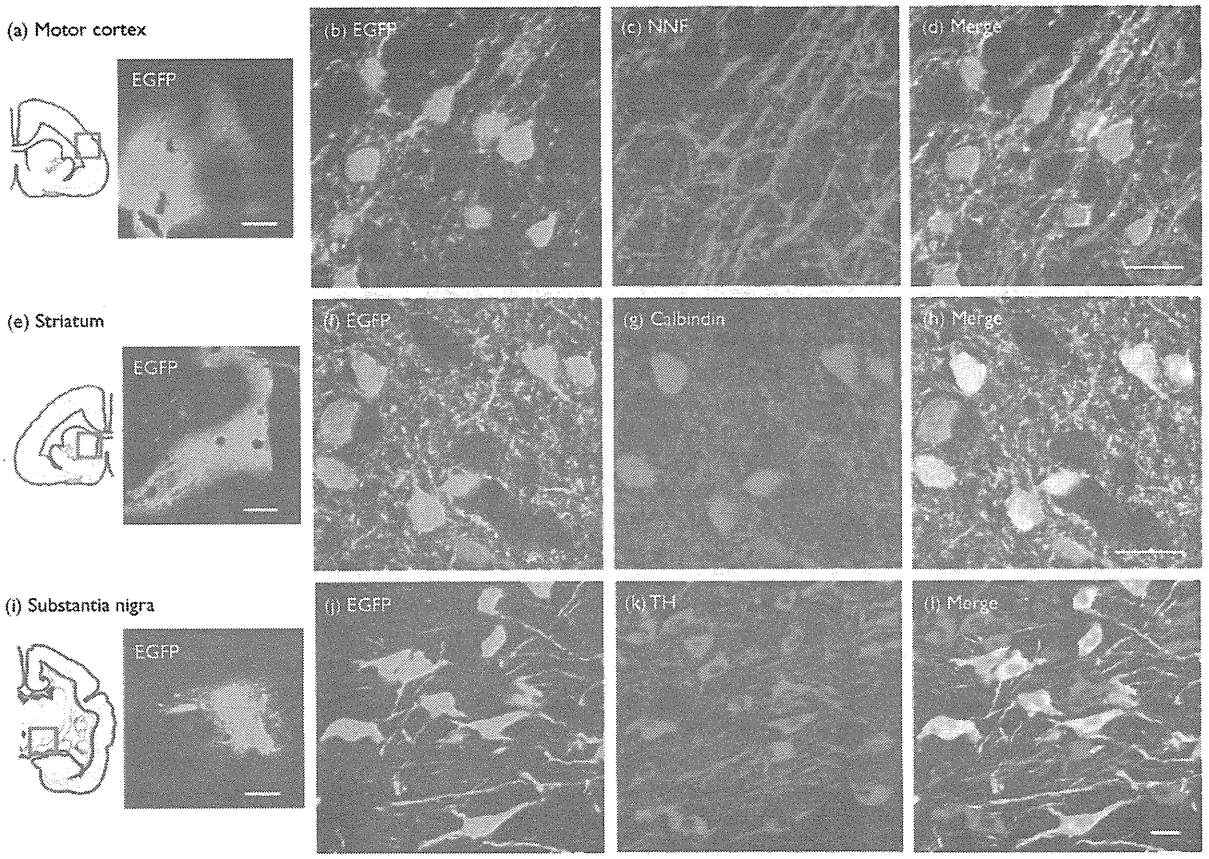

Identification of cell types of adeno-associated virus 8-infected neurons in the motor cortex, the striatum and the substantia nigra. Confocal images with a low-power field show native enhanced green fluorescent protein (EGFP) fluorescence at the three injection sites (a, e, i; green), approximately corresponding to the red boxes on the insets of coronal marmoset brain maps. High-power confocal images show $EGFP^+$ cells (green) in the motor cortex (b), the striatum (f) and the substantia nigra (j). $EGFP^+$ cells are colocalized with non-phosphorylated neurofilament protein (NNF, c; red), calbindin (g; red), and tyrosine hydroxylase (TH, k; red) as shown by the merged images (d, h, l; yellow). Bars represent 500 μm in (a), (e), (i), and 20 μm in (d), (h), (l).

Table 1 Quantification of infection efficiency in identified neuronal cell types after AAV8-EGFP virus injection

Injection site	Neuron (neuronal marker$^+$/ $EGFP^+$cells)	Astrocyte ($GFAP^+$/ $EGFP^+$cells)	Oligodendrocyte ($Olig2^+$/ $EGFP^+$cells)
Motor cortex	91% (169/185)	1% (2/189)	0% (0/197)
Striatum	98% (190/193)a 70% (142/202)b	0% (0/195)	1% (2/207)
Substantia nigra pars compacta	99% (190/192)	0% (0/193)	3% (5/190)

NNF in the motor cortex, NeuN (a) and calbindin (b) in the striatum, and TH in the substantia nigra were used as the neuronal marker.
AAV, adeno-associated virus; EGFP, enhanced green fluorescence protein; GFAP, glial fibrillary acidic protein; NeuN, neuron-specific nuclear protein; NNF, nonphosphorylated neurofilament protein; Olig2, oligodendrocyte transcription factor 2; TH, tyrosine hydroxylase.

$EGFP^+$ cells in each injected site were colocalized with neuron-specific markers. In contrast, we rarely found colocalization of EGFP fluorescence with specific marker proteins for glial cells. As we used a ubiquitous promoter (CAG promoter) in this study, the present results indicate endogenous AAV8 tropism for neurons, but not for glia, in marmoset brains *in vivo*. The neuronal tropism of AAV8 revealed in the present study is consistent with an earlier study in cynomolgus monkeys [24]. It has been shown that AAV8 could transfect astroglia in primary culture prepared from newborn rats, but rarely *in vivo* in rat hippocampus [25]. Therefore, the degree of neurotropism of AAV8 may depend on the infection conditions (*in vivo* vs. *in vitro*).

In the present study, we examined EGFP expression 4 weeks after injection of AAV8-EGFP. Eslamboli *et al.* [20] showed long-term (at least 1 year) transgene expression through AAV5 in the marmoset substantia nigra. Thus, it is likely that AAV8 also enables stable transgene expression in primate brains for long periods.